Memoirs of the School of Engineering, Nagoya University
Vol.51, No.1 (1999)

BEHAVIOR OF MULTISTAGE MIXER-SETTLER EXTRACTION COLUMN

Katsuroku TAKAHASHI and Susumu NII

Department of Chemical Engineering

(Received May 31, 1999)

Abstract

A counter-current multistage extraction column having high performance (i.e., high extraction efficiency and large maximum throughput) has been developed. The hydrodynamic behavior and the mass transfer characteristics of the column were analyzed experimentally. Each stage of the column consists of lower mixer part, upper settler part and a drop coalescer between them. Both of the continuous and the dispersed phases rise from the mixer into the settler and are seperated into two phases within the settler. The continuous phase goes down to the lower stage mixer through the downspout pipes and the dispersed phase rises to the upper stage mixer through the riser pipes. The maximum throughput in the column is independent of the drop size because the counter-current flow in the dispersion situation is avoided. Then the column can be operated at a strong agitation where the extraction efficiency is high due to large interfacial area with small drops. As the hydrodynamic behavior, the maximum throughput, the holdup of dispersed phase and the drop size were examined. The maximum throughput can be determined from the balance between the pressure drop within the downspout and the sum of the suction pressure induced by the impeller and the buoyant force of dispersed phase. The holdup of the dispersed phase in the mixer is given by a model of dispersed phase leaving the mixer, including the diffusional flow of dispersed phase. The drop size in the mixer depends on the residence time of the dispersed phase as well as the Weber number. The mass transfer characteristics can be expressed by a rigid sphere model of drop because the drop diameter is small at a strong agitation in the mixer. A theoretical model of diffusion within a rigid sphere gives the mass transfer coefficient in the dispersed phase, and the correlation by Ranz-Marshall for the mass transfer around a rigid sphere gives the mass transfer coefficient in the continuous phase. The extraction of copper with the five-stage mixer settler extraction column was represented by the calculation with the above hydrodynamic and mass transfer characteristics as well as the extraction reaction rate at the interface.

Keywords: extraction, extraction column, maximum throughput, holdup, drop size, mass transfer coefficients

Contents

1. Introduction 3

2. Mixer-Settler Extraction Column 4

3. Maximum Throughput in MS Column 5
3.1 Experimental 5
3.2 Results and Discussion 6
3.2.1 Throughput 6
3.2.2 Pressure differences 8
3.2.3 Estimation of throughput 9

4. Dispersed Phase Holdup within Mixer of MS Column 10
4.1 Experimental 11
4.2 Results and Discussion 11
4.2.1 Dispersed phase holdup in the mixer 11
4.2.2 Effects of interfacial tension and density difference 11
4.2.3 Model for dispersed phase holdup 14

5. Drop Size in MS Column 16
5.1 Experimental 16
5.2 Results and Discussion 17
5.2.1 Sauter mean diameter 17
5.2.2 Effect of residence time of dispersed phase on drop size 18
5.2.3 Drop size distribution 19

6. Mass Transfer Coefficients in MS Column 20
6.1 Experimental 20
6.2 Results and Discussion 21
6.2.1 Volumetric over-all mass transfer coefficient 21
6.2.2 Interfacial area 23
6.2.3 Over-all mass transfer coefficient 23
6.2.4 Dispersed phase mass transfer coefficient 24
6.2.5 Dispersed phase mass transfer coefficient based on rigid sphere model 25
6.2.6 Continuous phase mass transfer coefficient 28

7. Stage Efficiency in MS Column 30
7.1 Experimental 30
7.2 Results and Discussion 31
7.2.1 Stage efficiency 31
7.2.2 Effect of agitation speed, flow rates and distribution ratio on stage efficiency 33
7.2.3 Estimation of stage efficiency 35

8. Extraction of Copper by MS Extraction Column 38
8.1 Experimental 39
8.2 Results and Discussion 39
8.2.1 Copper extraction with MS column 39
8.2.2 Mass transfer coefficients in FISV 40
8.2.3 Copper extraction rate in FISV 41
8.2.4 Calculation of copper extraction within MS column 42

8.2.5 Specific interfacial area 44
8.2.6 Mass transfer coefficients within MS column 46
8.2.7 Extraction rate with purified extraction 46
8.2.8 Simulation for various conditions of extraction column 47

1. Introduction

The counter-current multistage extraction is useful to separate the mixed solution. Among many types of the extractor[1)], the multistage mixer-settler is widely used in industry because it gives a stable operation and high stage efficiency. However, it needs a large space because of the horizontal arrangement of stages. So, the column type extractor of high performance is desirable. Factors affecting the performance of extraction column are given in Fig.1. A large maximum throughput and high separation efficiency (stage efficiency) must be achieved to get a compact extraction column, i.e., the column with a small diameter and a small height. The stage efficiency depends on the interfacial area of dispersed phase and the mass transfer coefficients in the continuous and the dispersed phases. The interfacial area increases with the decrease in drop size and with the increase in holdup of the dispersed phase. The decrease in drop size also makes the dispersed phase holdup large due to the decrease in relative velocity between the dispersed drop and the continuous phase. However, for the column where phases flow counter-currently in the dispersed situation, the flooding follows this decrease in relative velocity, which makes the maximum throughput small. The column without mechanical agitation, such as the spray column or the packed column, has large throughput but small interfacial area because of large drop size. Mechanical agitation, such as in the MIXCO column, RDC column[2)] or Kuhni column[3)], makes the stage efficiency high due to the large interfacial area, but the throughput small. Besides, the axial

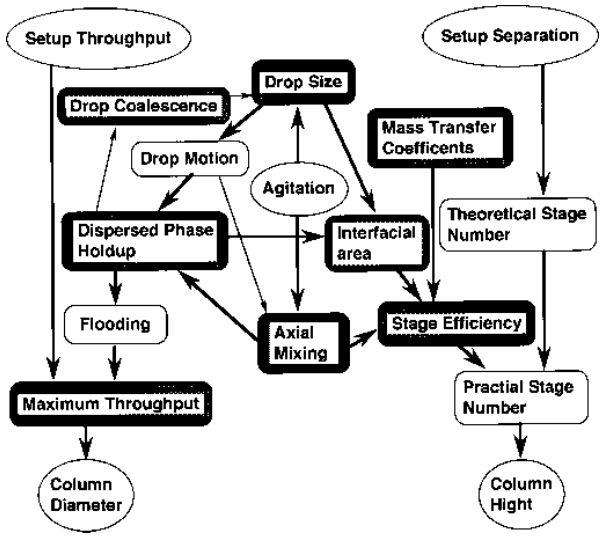

Fig.1 Factors affecting performance of extraction column

mixing between stages becomes appreciable at a large agitation speed and it makes the stage efficiency low. The behavior of the dispersed phase holdup is complex because it depends on the drop size, the flow rates of both phases and the mixing degree in the mixer[4]. When drop coalescence occurs in the mixer, the drop size is affected by the holdup, which makes the holdup behavior more complex[5]. This complex behavior makes the analysis of extraction column difficult because the holdup influences the interfacial area as well as the maximum throughput. The stereopartition between stages used in the Sheibel column[6,7], EC column[8] or SHE column[9] suppresses the axial mixing and makes the throughput large by drop coalescence within the partition. The electrostatic drop coalescence between stages is effective to obtain stable operation under vigorous agitation[10]. Within the mixer-settler column, the partition is stronger and drops coalesce more completely within the settler. The maximum throughput of the mixer-settler column does not depend on the drop size, i.e., the throughput does not decrease with the agitation speed.

2. Mixer-Settler Extraction Column

Treybal proposed a rectangular mixer-settler tower with the horizontal arrangement of the mixer and the settler in each stage, i.e., each stage in the mixer-settler extractor is piled up in vertical direction[11]. The Wirz column has a mixer at the center of the column and a settler around the mixer[12,13]. The MIXET column has vertical arrangement of the mixer and the settler[14]. This column gives high stage efficiency but a small throughput because flow channels of the continuous and the dispersed phases are not separated. The asymmetric rotating disc column is a kind of mixer-settler column[15,16].

We proposed a mixer-settler extraction column (MS column)[17] shown in Fig. 2. One stage of the column consists of a lower mixer part and an upper settler part, and a drop coalescer is set between them. The coalescer is a three-dimensional lattice made of glass fiber mesh coated with PTFE, and is 12 mm in height and 2.5×2.3 mm rectangular pitch. A lifter-turbine impeller having paddles below a disc is used for agitation in the mixer. Continuous phase (aqueous phase) fed to the mixer of top stage rises through the drop coalescer into the settler with the dispersed phase, goes down through the downspouts into the lower stage mixer after settling into two phases and finally is led to the leveler from the bottom of the column. While dispersed phase (organic phase) fed at the bottom of the column rises into the mixer of bottom stage through the risers, from the mixer into the settler through the drop coalescer with the continuous phase, from the settler into the upper stage mixer and finally overflows from the top of the column. The downspouts of continuous phase act as the baffles in the mixer.

The characteristics of the MS column are as follows.

1. The maximum throughput increases with the agitation speed, and a large throughput and high stage efficiency is realized simultaneously.
2. The effect of liquid mixing between stages is small.
3. The mass transfer resistance becomes small by repeating the dispersion and the coalescence of drops.
4. Suction pressure induced by a lifter-turbine impeller promotes the dispersed phase flow resulting a large throughput.
5. Analysis of the column is easy because the stages are independent each other.

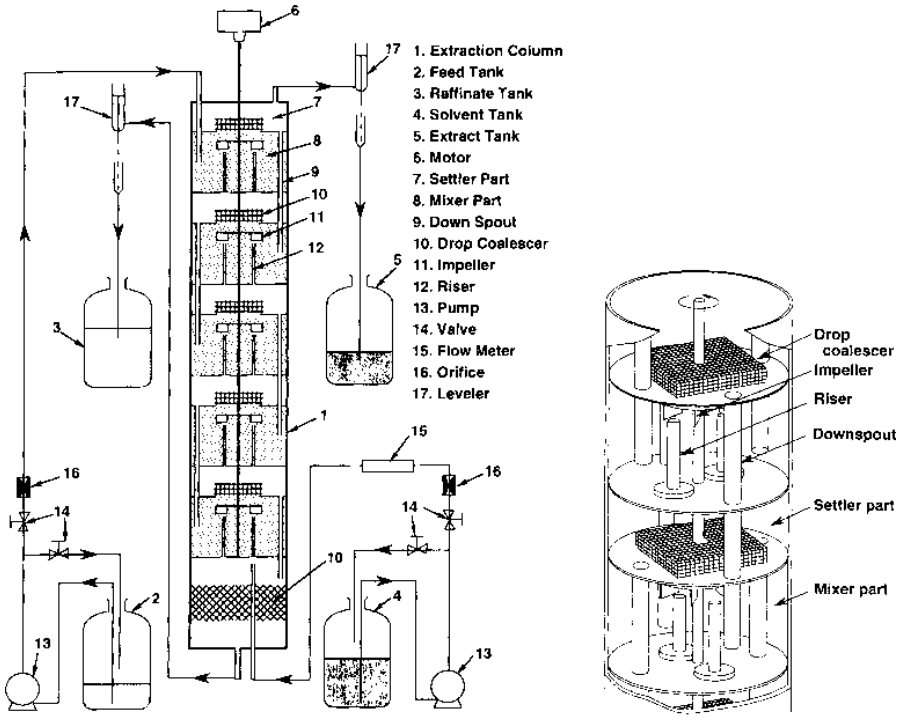

Fig.2 Diagram of mixer-settler extraction column

3. Maximum Throughput in MS Column

For the extraction column in which two phases flow counter currently in the dispersion situation, the maximum throughput depends on the drop motion relative to the continuous phase. It is difficult to estimate the maximum throughput because the drop motion, which depends on the drop diameter, the mixing degree and the flow rates, is very complex. On the other hand, the maximum throughput in the MS column is determined by the different mechanisms because two phases flow concurrently in dispersed situation from the mixer to the settler.

The throughput has been measured for the MS columns of 60[17] and 100[18] mm column diameter and the effects of the internals on the throughput was investigated. To elucidate the behavior of the throughput, the pressure differences between several points in the column were also measured. The factors affecting the throughput will be discussed, and it will be shown that the maximum throughput can be estimated rationally.

3.1 Experimental

The columns are made of acrylic resin pipe of 60 and 100 mm inner diameter. The column of 100 mm diameter has five stages and a drop coalescer at the bottom of the column as shown in Fig.2. Each stage consists of a mixer part of 60 mm height and a settler part of 40 mm height. A lifter-turbine impeller having 6-paddle under a disk of 50 mm diameter agitates in the mixer. A drop coalescer is set on a stator ring of 50 mm opening diameter between the mixer and the settler.

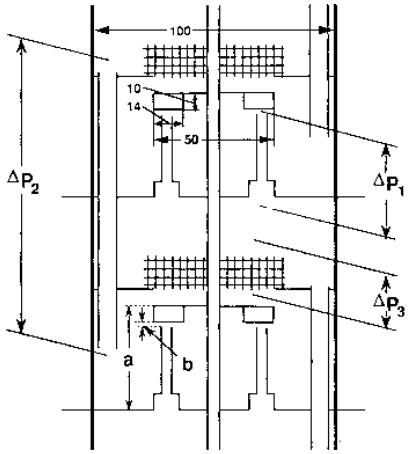

Fig.3 Measured point of pressure difference

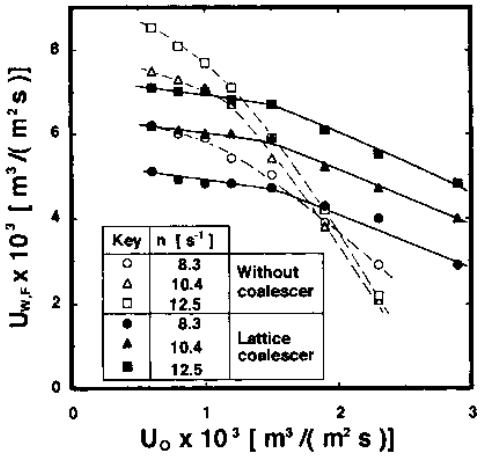

Fig.4 Effect of coalescer on maximum throughput

Downspouts from the settler to the lower stage mixer are made of glass tubes of 9.6 mm inner diameter and glass tubes of 7.6 or 5.6 mm inner diameter are also used in some experiments. Risers from the settler to the upper stage mixer are made of PTFE pipes of 6 mm inner diameter.

The measurement of the throughput was carried out as follows. As the continuous phase (water) flow rate was gradually increased under a constant flow rate of organic phase (heptane), an accumulated layer of heptane appeared at the top of the settler and the amount of the layer increased rapidly with a small increase in water flow rate. When the layer height reached 10 mm, the water flow rate was measured by receiving water from the leveler with a measuring cylinder for a given time and the flow rate was regarded as a flooding flow rate. The effects of internals on the throughput were measured for third stage by changing diameter of the downspout, distance between the impeller and the riser, *b*, and position of the impeller from the bottom of the mixer, *a*, shown in Fig.3. In the present MS column, hydrodynamic characteristics in one stage was not affected by other stage internals.

Pressure differences at various points were also measured, i.e., ΔP_1 was pressure difference between ends of riser, ΔP_2 between ends of the downspout and ΔP_3 across the drop coalescer as shown in Fig.3. In these measurements the dispersed phase was not fed and the risers were plugged up. The plugging would make the situation that was corresponding to the stop of dispersed phase flow by the flooding.

3.2 Results and Discussion

3.2.1 Throughput

Effect of the drop coalescer on the maximum throughput is shown in Fig.4, where the maximum flow rates, $U_{W,F}$, of water are plotted against the flow rate,U_O, of heptane. Without coalescer, $U_{W,F}$ is large at small U_O and it decreases rapidly with the increase in U_O, especially at large agitation speed, *n*. When the coalescer is set, the operation is stable at large U_O. In this case a plane interface was observed within the settler, while drops were accumulated in the settler for the absence of the coalescer. Mesh sheet and urethane foams are tested as a drop coalescer. Heptane stayed at the horizontal mesh sheet and plugged the mesh openings. The value of $U_{W,F}$ for the

mesh coalescer was smaller than that for the lattice coalescer. When urethane foam was used as a coalescer, $U_{W,F}$ decreased with the decrease in the opening diameter of the foam. The lattice coalescer was superior to the foam coalescer of 4.5 mm opening diameter. The vertical yarn in the lattice coalescer seems to act effectively for the dispersed phase flow within the coalescer.

The maximum flow rates of water, $U_{W,F}$, for various columns are shown in Fig.5 for $U_O = 5 \sim 6 \times 10^{-4}$ m^3/(m^{2}s). The throughput for the MIXCO column is given as the general behavior of the extraction column, which decreases with the increase in agitation speed, n. On the other hand, $U_{W,F}$ for MS column increased linearly with n. Since the specific interfacial area increases with n

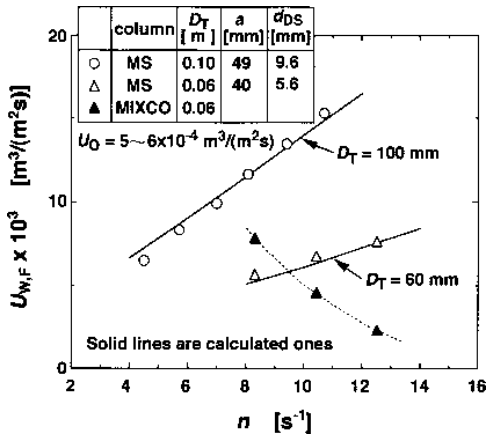

Fig.5 Maximum flow rate of continuous phase for various columns

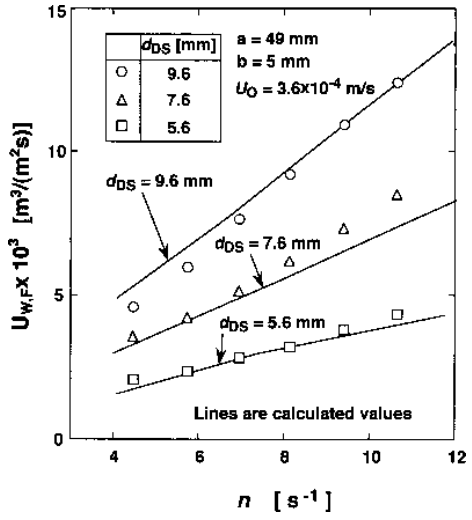

Fig.6 Effect of downspout diameter on maximum flow rate

because of the decrease in dispersed drop diameter, the mass transfer efficiency is improved with the increase of n[19]. Therefore, the increase of the throughput with n can offer the extraction column a favorite characteristic, i.e., both high mass transfer efficiency and large throughput can be realized. The increase of $U_{W,F}$ with n may be caused by the suction pressure induced by the lifter-turbine impeller as will be described later. Value of $U_{W,F}$ for 100 mm column was 2.3 times as large as those for 60 mm column, i.e., scale-up effect was very large.

The distance, b, between the impeller and the riser is important for $U_{W,F}$. For any value of b, $U_{W,F}$ increased linearly with n, and it decreased with the increase in b. The value of $U_{W,F}$ decreased largely with the change in b from 1 to 5 mm, and the difference in $U_{W,F}$ between b = 10 and 20 mm was very small. When b increased beyond a/2, $U_{W,F}$ decreased largely again and the value at b = 30 mm was about half of that at b = 1mm. The effect of impeller position, a, on $U_{W,F}$ was not so much. The increase rate of $U_{W,F}$ with n became large with the decrease in a. The fact that large $U_{W,F}$ can be realized with small a is favorable to decrease the column height.

Figure 6 shows the effect of inside diameter, d_{DS}, of the downspout on $U_{W,F}$. The value of $U_{W,F}$ decreases largely with the decrease in d_{DS}. This is because of pressure drop of water flow through the downspout which increases with the decrease in d_{DS} as will be described later.

3.2.2 Pressure differences

The dispersed phase flows by the pressure difference between ends of riser. The effects of agitation speed, n, and water flow rate, U_W, on the pressure difference, ΔP_1, between ends of the riser is shown in Fig.7. Negative value of ΔP_1 indicates that the pressure beneath the impeller is lower than that in the settler of lower stage. ΔP_1 for U_W = 0 is negative because of the suction by the lifter-turbine impeller and the pressure difference is regarded as P_S (= $-\Delta P_{1,Uw=0}$). As U_W increases, ΔP_1 increases because of the increase in the pressure drop, ΔP_f, since ΔP_1 is given by $\Delta P_f - P_S$. When dispersed phase is fed and U_W approaches $U_{W,F}$, the riser may be filled with dispersed phase and the buoyant force, P_h (= $\Delta\rho gh$), plays positively for the dispersed phase flow through the riser as well as P_S. As the result, the dispersed phase stops flowing when ΔP_f reaches

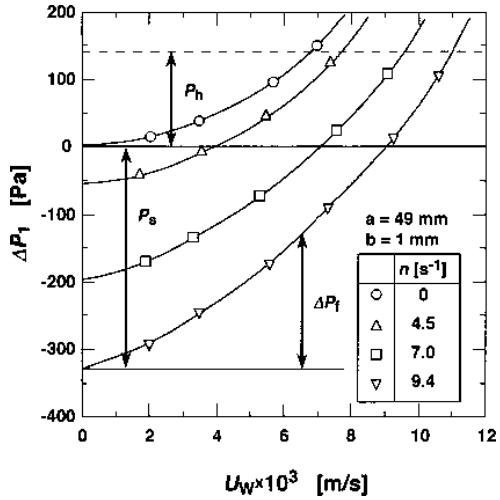

Fig.7 Pressure difference between ends of riser

$P_S + P_h$, that is, U_W in this situation is $U_{W,F}$.

The suction pressure induced by the lifter-turbine impeller increased with the impeller diameter, D_i, as well as the agitation speed, and correlated with $n D_i$ for b = 1mm as follows.

$$P_S = 2200(n D_i - 0.15)^{1.5} \quad (1)$$

This correlation can not be used for $n D_i < 0.15$ where P_S is negligibly small. The value of P_S varied a little with the radial distance, and it became maximum for r = 13 ~ 19 mm in case of D_i = 50 mm, i.e., the position between inner end and center of the paddle. Risers were set at this radial position. The pressure drop ΔP_f can be given by ΔP_1 for n = 0, which increases linearly with U_W^2. For the section corresponding ΔP_1, water flows from the mixer to the settler across the coalescer, from the settler to the lower stage mixer through the downspout and from the mixer to the settler across the coalescer in the lower stage, i.e., through one downspout and two coalescers. The pressure drops for the downspout, ΔP_2, was about 95 % of ΔP_1 and $2\Delta P_3$ only 5 % of ΔP_1.

Pressure drops, ΔP_2, for downspout is given by the pressure drop within a pipe as follows [20].

$$\begin{aligned} \Delta P_2 &= \Delta P_{inlet} + \Delta P_{pipe} + \Delta P_{outlet} \\ &= \zeta(\rho u_{DS}^2 / 2) + 4f(l/d)(\rho u_{DS}^2 / 2) + \rho(u_{DS} - u_{out})^2 / 2 \end{aligned} \quad (2)$$

Where ζ is inlet coefficient of pressure drop, f friction factor and l/d ratio of pipe length to inside diameter. The flow velocity within downspout, u_{DS}, is given by $U_W(D_T/d_{DS})^2/2$, and the velocity, u_{out}, at the outlet of downspout can be assumed to be zero. The value calculated by Eq.(2) with ζ = 0.5 coincides with the experimental values.

3.2.3 Estimation of throughput

For small flow rate of dispersed phase, $U_{W,F}$ can be determined to satisfy the following relation as mentioned above.

$$P_S + P_h = \Delta P_f = \Delta P_2 + 2\Delta P_3 \quad (3)$$

By using Eq.(1) for P_S, Eq.(2) for ΔP_2, $P_h = \Delta\rho gh$ where h is a height of dispersed phase accumulated within the riser and at the top of the settler, and $2\Delta P_3 = 1.22 \times 10^5 U_W^2$ obtained from experimental measurement, $U_{W,F}$ was determined to satisfy Eq.(3) and shown in Fig.5 with solid lines. For small column (D_T = 60 mm), since the downspout pipe protruded about 5 mm from the bottom of the settler, ζ = 2.0 was used as a medium value between 1.3 ~ 3.0[20]. The calculated results well reflected the change in $U_{W,F}$ with n.

The values of $U_{W,F}$ in Fig.6 measured for b = 5 mm might be smaller than those for b = 1 mm because of the decrease in suction pressure P_S with b. Then P_S for b = 5 mm was assumed to be 3/4 of that for b = 1 mm, and $U_{W,F}$ for various inside diameters of downspout were calculated and shown with solid lines in Fig.6. These calculated results agreed well with the experimental results. The comparison of the calculated $U_{W,F}$ with the experimental ones in Figs.5 and 6 indicates that $U_{W,F}$ can be estimated rationally by Eq.(3).

For the columns of similar structural figures, the calculated throughput at a same agitation speed increased in proportion to the column diameter, D_T. The dispersed drops, however, may be smaller with a larger impeller for same agitation speed, and small drops can not be coalesced completely within the coalescer, which is followed by unstable operation because dispersed phase is

accompanied with the continuous phase and adheres to the wall of the downspout. By using the correlation for the sauter mean drop diameter in the MS column[21], the agitation speeds corresponding to a given drop diameter were calculated for various column diameters. Though the throughput for a given drop diameter increases with the column diameter, the increase rate is not so large. The throughput varied largely with the diameter of downspout as shown in Fig.6. Enlarging the downspout diameter may be effective to get a large throughput. The value of $U_{W,F}$ for enlarged downspout diameter and a fixed impeller diameter, where the column diameter is also enlarged to insert large downspouts, was calculated. The calculated throughput for d_{DS} = 20 mm is 2.5 times as large as that for d_{DS} = 10 mm. Since the drop diameter is expected to be large for large D_T/D_i from the measurement with the agitation vessel, large agitation speed can be adopted for the column of large D_T/D_i. The throughput of 150 $m^3/(m^2hr)$ (= 0.0417 $m^3/(m^2s)$), which is larger than the reported value for any extraction column, is expected to be realize with the column of d_{DS} = 20 mm.

In the present experimental system, interfacial tension was large and large agitation speed could be used. For the system of small interfacial tension, agitation speed must be small to coalesce the dispersed drops completely, because the drop diameter decreases with the decrease in interfacial tension. Under agitation speed where the sauter mean drop diameter is 0.2 mm, the throughputs were calculated for various interfacial tensions. The calculated value of $U_{W,F}$ decreased with the decrease in interfacial tension. On the other hand, the density difference, $\Delta\rho$, between the dispersed and the continuous phases is considered to affect the throughput. The effect of density difference for the present MS column is expressed by the term $P_h = \Delta\rho gh$. The calculated variation of $U_{W,F}$ with $\Delta\rho$ was comparatively small. This is because of the fact that $U_{W,F}$ depends on not only P_h but also P_S as expected from Eq.(3) and the effect of P_S on $U_{W,F}$ is dominant at a large n.

Maximum throughput of the mixer-settler extraction column increased linearly with the agitation speed and the value for the 100 mm column was 2.3 times as large as that for the 60 mm column. The throughput was largely affected by the diameter of downspout as well as the distance between the impeller and the top of riser. From the measurement of pressure difference between ends of riser, it was indicated that the throughput is determined from the balance among the pressure drop, ΔP_f, of fluid flow, suction pressure, P_S, induced by the lifter-turbine impeller and the buoyant force, P_h. The suction pressure P_S for the distance between the impeller and the riser b = 1 mm was correlated by Eq.(1) with the tip velocity of the impeller. The greater part of ΔP_f was the pressure drop through the downspout which could be calculated by Eq.(2). By using these equations, the maximum throughput could be determined to satisfy Eq.(3). The calculation indicated that the throughput increased largely with the downspout diameter and with the column diameter for the column of similar figures. The decrease in interfacial tension results in the decrease of throughput, while the density difference between the dispersed and the continuous phases affected a little the throughput.

4. Dispersed Phase Holdup within Mixer of MS Column

The holdup of the dispersed phase as well as the drop size is used to determine the interfacial area. Therefore, it is never dispensable in the analysis or estimation of mass transfer within the extraction column. The estimation of the holdup in the extraction column having mechanical agitation and counter-current flow in the situation of drop dispersion is difficult because it depends on the drop motion, agitation strength and the flow rates.

The holdup of the dispersed phase was measured in a single-stage MS column, and a simple model to predict the dispersed phase holdup has been developed based on the holdup profile in the

vertical direction in the mixer. The model parameters are correlated with the agitation speed, interfacial tension and the density difference between the dispersed and the continuous phases[22].

4.1 Experimental

The experimental apparatus used in this work is a single-stage MS column having a lower mixer and an upper settler. The column diameter is 100 mm, the mixer height 60 mm, the settler height 40 mm and the impeller diameter 50 mm. The holdup in the mixer was measured by drawing out a liquid sample with a syringe having pipe parts of 1.7 mm inner diameter and 200 mm length and of 13 mm inner diameter and 70 mm length. The syringe was inserted into the mixer through a sampling tube located 40 mm from the column axis. The total amount of liquid sample was taken into the large diameter section of the syringe and settled to separate the organic phase from the aqueous phase. After measuring the sample weight, W_T, the organic phase was moved slowly to the small diameter section of the syringe by discharging the aqueous phase. The volume of the organic phase, V_O was determined from the tube length occupied by the organic phase, and the dispersed phase holdup, ϕ, was calculated by the following equation.

$$\phi = V_O \,/\, [\{(W_T - V_O\rho_O)\,/\rho_W\} + V_O] \tag{4}$$

Where ρ_O and ρ_W are densities of the organic phase and the aqueous phase, respectively.

The organic phase used in the experiments was heptane, tributyl phosphate (TBP) - heptane solution or cyclohexane; aqueous phase was deionized water. TBP is an extractant used for the extraction of various metal ions. All the experiments were carried out at the room temperature of $25 \pm 1^{\circ}$C.

4.2 Results and Discussion

4.2.1 Dispersed phase holdup in the mixer

Local holdup, ϕ, of the dispersed phase in the mixer is shown in Fig.8 against the vertical distance, H, from the bottom of the mixer for the dispersed phase of heptane. The value of ϕ below the lifter turbine (LT) impeller does not vary with H, but ϕ decreases suddenly near the lower end of the impeller. Although the same change in ϕ near the impeller is observed for the disc turbine (FBT) impeller, it is smaller than that for the LT impeller. The holdup for the LT impeller is much larger than that for the FBT impeller at the same agitation speed of $n = 8\ s^{-1}$, as is seen in Fig.8. Hence the LT impeller is superior in achieving a large interfacial area because the area increases both with the increase in the holdup and with the decrease in the drop size which decreases with the residence time of the dispersed phase[21]. The remaining experimental runs were made by use of the LT impeller, and holdups were measured at two positions below (H = 3 cm) and above (H = 5.2 cm) the impeller where ϕ varied little with H.

The holdup, ϕ^L, in the lower part of the mixer is shown against n for various flow rates, q_O, of organic phase and q_W, of aqueous phase in Fig.9. The value of ϕ^L increases with n and q_O, but q_W has a reverse effect on ϕ^L; the effect of q_O is larger than that of q_W. On the other hand, the holdup, ϕ^U, in the upper part of mixer also increases with n and q_O.

4.2.2 Effects of interfacial tension and density difference

The motion of dispersed drop depends on the drop diameter and the density difference, $\Delta\rho$, between the continuous and the dispersed phases, while the drop diameter in the agitated vessel changes with the interfacial tension. Therefore, the holdup of the dispersed phase is expected to vary with interfacial tension and density of the dispersed phase when the continuous phase is an

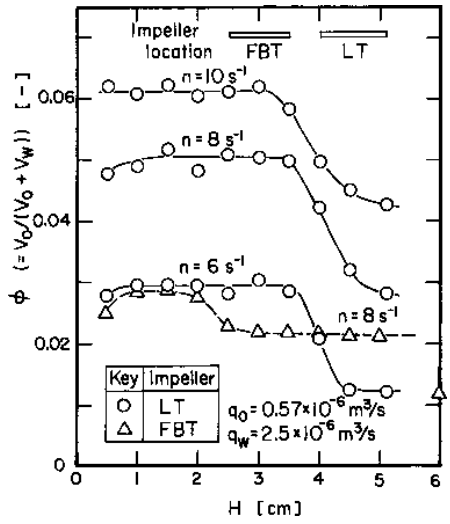

Fig.8 Holdup profile of dispersed phase in vertical direction of mixer

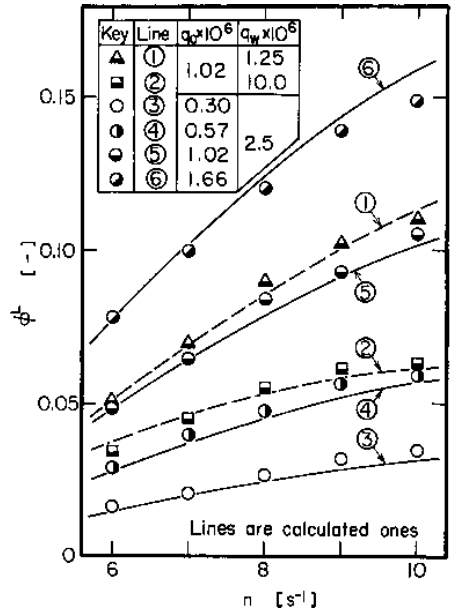

Fig.9 Holdup of dispersed phase in lower part of mixer

aqueous solution. Thus, adding TBP to heptane varied the two physical properties. In the presence of a small amount of TBP the interfacial tension, γ, between the organic phase and water is reduced remarkably, while the density difference varied linearly with TBP concentration. The effects of TBP concentration on ϕ^L and ϕ^U are shown in Fig.10 and 11, respectively. Both holdups increase with the increase in TBP concentration because of the decreases in interfacial tension and density difference.

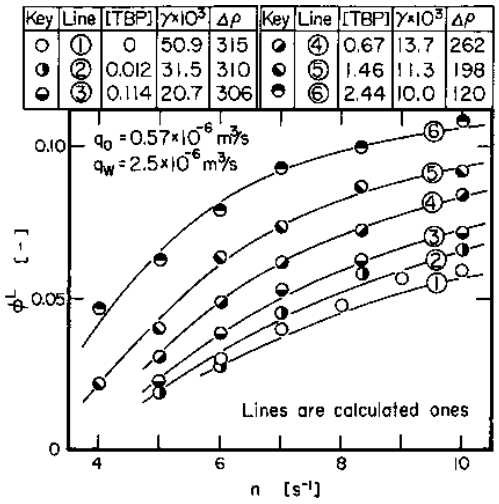

Fig.10 Holdup of dispersed phase in lower part of mixer for various TBP concentrations in organic phase

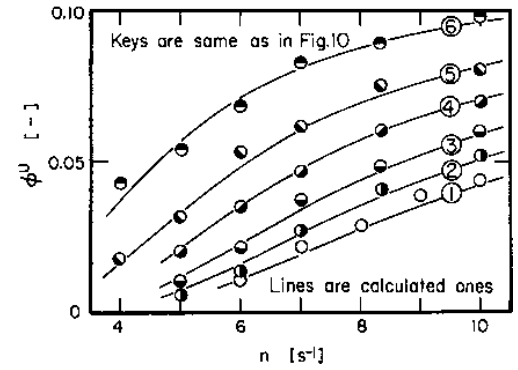

Fig.11 Holdup of dispersed phase in upper part of mixer for various TBP concentrations in organic phase

4.2.3 Model for dispersed phase holdup

In the lower part of the mixer, both the dispersed and the continuos phases are circulating between the core region and the circumference of the mixer, flowing out through the space around the impeller at the flow rate $q_O + q_W$. The holdup ϕ^L may be dependent on the discharge mode of the dispersed phase from the lower part to the upper part of the mixer. Besides the discharge of the dispersed phase by axial flow through the space around the impeller, a diffusional transfer, depending on a difference in the local holdup gradient near the lower end of the impeller as can be seen in Fig.8, may exist. Then it was assumed that the discharge rate of the dispersed phase could be expressed as follows.

$$q_O = (q_O + q_W)\,\phi^L + KA\,(\phi^L - \phi^U) \tag{5}$$

Where K is the transfer coefficient and A is cross-sectional area of flow pass around the impeller, i.e., the area obtained by subtracting the cross-sectional area of four pipes and the area occupied by the impeller from the cross-sectional area of the column (A = 0.00558 m^2 in this work). The value of K was evaluated from Eq.(5) with ϕ^L and ϕ^U values shown in Fig.10 and 11, and shown in Fig.12. The value of K is independent of TBP concentration, i.e., the interfacial tension or the density difference, and it is also independent of flow rate given in Fig.9. The following correlation is derived from Fig.12.

$$K = 0.0043 + 260n^{-7} \tag{6}$$

The second term of right side in Eq.(6) may express the effect of large rising velocity for large drop at small n.

In the upper part of the mixer, the motion of dispersed drops would follow a free rising pattern because of the absence of circulating flow above the LT impeller. Therefore, the holdup of the dispersed phase may be expressed in a similar way as that in a spray column. Since the dispersed and the continuous phases flow concurrently through the mixer, the relative velocity, v_S, between the phases is given as follows[23].

$$v_S = [(q_O / \phi^U) - \{q_W / (1 - \phi^U)\}] / A \tag{7}$$

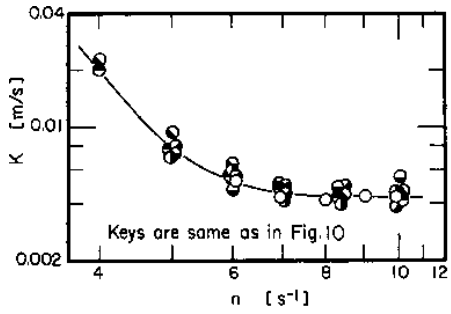

Fig.12 Transfer coefficient of dispersed phase for various TBP concentration in organic phase

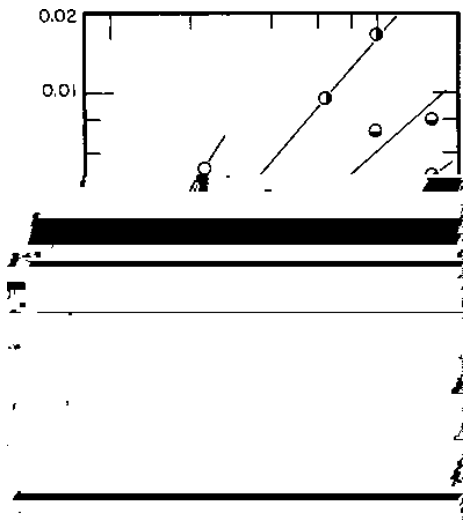

Fig.13 Relative velocity between dispersed and continuous phases

In Fig.11, the increase in ϕ^U with the concentration of TBP may be due to the change in γ for [TBP] < 0.114 kmol/m^3, and that in $\Delta\rho$ for [TBP] > 0.67 kmol/m^3. Since the γ-dependence of v_S obtained from ϕ^U in Fig.11 was nearly equal to the $\Delta\rho$-dependence for constant n, values of v_S are plotted against the product of $\Delta\rho$ and γ in Fig.13. A linear relation has been obtained for each agitation speed. The product, $\Delta\rho\gamma$, mainly depends on $\Delta\rho$ at smaller $\Delta\rho\gamma$ and on γ at larger $\Delta\rho\gamma$. Kumar et al.[3] reported that v_S in the Kuhni-type extraction column was proportional to γ. In Fig.13, v_S is proportional to $\Delta\rho\gamma$ (i.e., γ at large $\Delta\rho\gamma$), when n is around 5 s^{-1}. The dependency of v_S on $\Delta\rho\gamma$ varies with n; hence v_S is correlated as follows.

$$v_S = 0.00029\,(3.3\Delta\rho\gamma)^b, \quad where \;\; b = 0.2 + 13n^{-1.65} \tag{8}$$

Values of ϕ^U calculated from Eq.(7) with v_S by Eq.(8) are shown in Fig.11 by solid lines, while ϕ^L, calculated from Eq.(5) with ϕ^U and K of Eq.(6), is shown in Figs.9 and 10 by solid and broken lines. From the comparison of the experimental results with the calculated ones in Fig.9, it was found that the present model well describes the change in ϕ^L with the flow rate of the continuous phase as well as that with the flow rate of dispersed phase. For the other system of cyclohexane-water, a comparison of calculated ϕ^L values with the experimental results is given in Fig.14. In this case the effect of q_O or q_W on ϕ^L can also be explained by the present model.

Holdup distribution of the dispersed phase in the mixer part of the MS column was measured in a single-stage column having a LT or FBT impeller. For the LT impeller, a large difference in the holdups between below and above the impeller was observed. Then a diffusional transfer model of dispersed phase was proposed to express the holdup in the lower part of the mixer, and the holdup in the upper part was related to the relative velocity between the dispersed and the continuous phases. The transfer coefficient and the relative velocity as the model parameters were correlated with agitation speed, interfacial tension, and density difference between phases. Good agreement between calculated and experimental holdup was obtained for various flow rates of the dis-

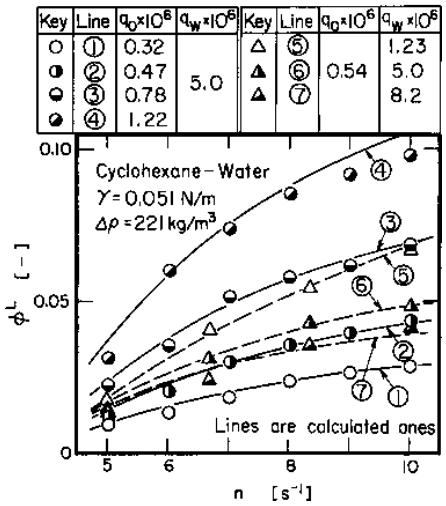

Fig.14 Comparison of calculated holdup of dispersed phase in lower part of mixer with experimental values measured for cyclohexane-water system

persed phase and the continuous phase.

5. Drop Size in MS Column

The drop size is used to determine the interfacial area as well as the dispersed phase holdup. In the general extraction column[24], e.g., the MIXCO column[2,4], the Kuhni column[4,25] or the RDC column[25], the drop size varies with the column height (stage number). It makes the column behavior complex and the analysis of extraction column difficult, because the dispersed phase holdup varies with the change in drop size. On the other hand, the drop sizes in the MS column does not vary with the column height because the stages in the MS column are independent each other.

The drop size in the MS column was measured with a single stage column[21]. Effects of the agitation speed, the interfacial tension and the residence time of the dispersed phase in the mixer are examined, and the drop size distribution is also discussed.

5.1 Experimental

The experimental apparatus is same as used in the measurement of dispersed phase holdup, i.e., the column of 100 mm inner diameter. The drop size was measured by photography through the column wall. A small mirror reflecting the light from a stroboscope was located at the level of impeller and 40 mm distance from column axis by the same way as Imai *et al.*[26]. The magnification of photograph was between 22 and 60. The diameters of about 1000 drops were measured for each run. The organic phase used in the experiments was TBP-heptane solution and the aqueous phase was deionized water. The interfacial tension was varied by the TBP concentration, and the residence time of the dispersed phase was varied by the continuous phase flow rate. All the experiments were carried out at room temperature of $25 \pm 1^{\circ}$C.

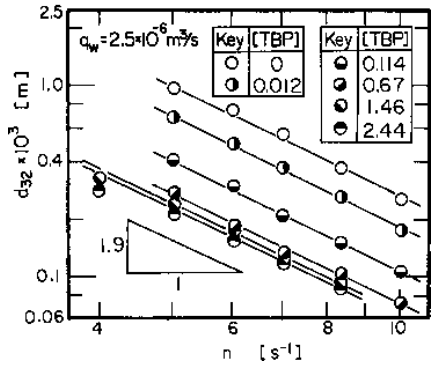

Fig.15 Sauter mean drop diameter against agitation speed

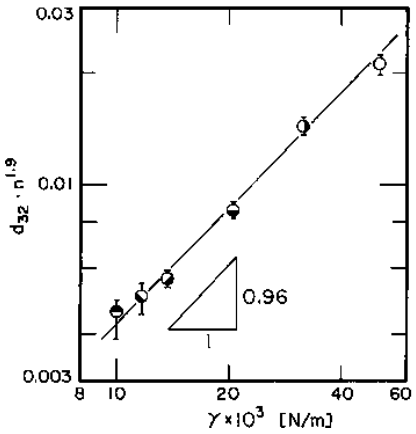

Fig.16 Effect of interfacial tension on Sauter mean diameter

5.2 Results and Discussion

5.2.1 Sauter mean diameter

Sauter mean diameters, d_{32}, of dispersed drops are plotted against the agitation speed in Fig.15. The value of d_{32} for each concentration of TBP decreases with the increase in n, and the slope is –1.9. This dependency of d_{32} on n coincides with that obtained by the batch stirred vessel under existence of surfactant[27] where the coalescence of drops in the vessel can be neglected. In the present experiment, the drop coalescence may hardly occur because the holdup of dispersed phase was very small. As the increase in the TBP concentration, d_{32} in Fig.15 decreases because of the decrease in the interfacial tension. The value of $d_{32} \cdot n^{1.9}$ is plotted against the interfacial tension in Fig.16, and a linear relation of slope of 0.96 is obtained. Since the absolute value of the slope in Fig.15 is just twice of that in Fig.16, d_{32} can be correlated with Weber number, We (= $D_i^3 n^2 \rho/\gamma$), as follows.

Where D_i is the impeller diameter. For the agitation vessel, the dependency of drop size on We number was derived to be –0.6 by Hinze[28)]

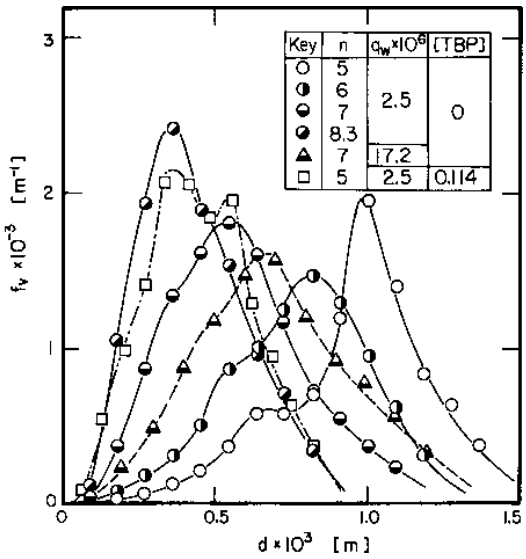

Fig.18 Volumetric drop size distribution

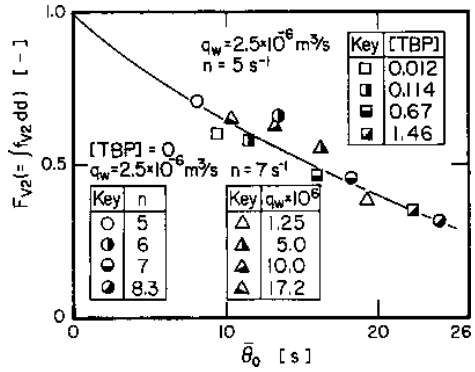

Fig.19 Fraction of second peak in drop size distribution against average residence time of organic phase

The absolute value of dependence of d_{32}/D_i on We number becomes smaller than in Eq.(9), but it is still larger than 0.6 derived theoretically by Hinze.

5.2.3 Drop size distribution

Volumetric drop size distribution of the dispersed drops in the mixer of the MS column is shown in Fig.18. At a small agitation speed, two peaks are observed in the distribution. When the distribution is divided into two single peak distributions under an assumption that the first distribution (smaller drops) is symmetric, the first one is given by normal distribution and the second one by a logarithmic normal distribution. The fractions, F_{V2}, of the second distribution to the total

distribution are given against θ_O in Fig.19. The value of θ_O was varied by three methods: by the agitation speed, by the TBP concentration and the flow rate of continuous phase. In any case, F_{V2} decreases with θ_O, that is, the fraction of the first distribution increased with the holdup ϕ^L. This indicates that the drops of the first distribution may be the circulating ones within the mixer and suffer several times breakage, because the increase in the circulating drops results in the increase of ϕ^L. The drops of the second distribution may be generated by the initial breakage of the inlet-dispersed phase, whose distribution is given by a logarithmic normal distribution like as the spray dispersion[39].

The drop size in the MS column varies with the residence time of the dispersed phase as well as the agitation speed and the interfacial tension between phases; it is correlated by Eq.(11). The drop size distribution has two peaks and the fraction of the first peak for small drop increases with the residence time of dispersed phase.

6. Mass Transfer Coefficients in MS Column

To design the extraction column, the mass transfer characteristics must be also known. In the usual extraction column, the diameter of dispersed drops and the dispersed phase holdup depend on the vertical position of the column[2-4], and the accurate estimation of these variations is difficult[40]. This makes it difficult to determine the mass transfer coefficients in the extraction column. On the other hand, the partition between stages in the MS column is more complete than those in other extraction columns, and the hydrodynamic behavior in one stage may not be affected by those in other stages, i.e., the behavior is independent for each stage. The Sauter mean drop diameter in the Wirz column does not change with the stage number[41] and flooding in the MS column occurs simultaneously in every stage[18]. This independence of each stage makes the analysis of mass transfer behavior simple.

The volumetric mass transfer coefficients of the MS column were measured with a single stage column[42], and the mass transfer coefficients of both dispersed and continuous phases were determined by use of the interfacial area estimated from the Sauter mean drop diameter[21] and the dispersed phase holdup[22]. These coefficients were compared with theoretical values and with mass transfer coefficients obtained from a rigid sphere correlation.

6.1 Experimental

Experimental apparatus used in this work is a single stage MS column that is the same as in the previous paper[22]. This corresponds to one stage of the MS column shown in Fig.2, and both inner column diameter and column height are 100 mm. The column is divided into a mixer part of 59 mm height and a settler part of 38 mm height by a stator ring of 3 mm thickness having 50 mm opening. A drop coalescer, a three dimensional lattice of 12 mm height and 2.5×2.3 mm rectangular pitch made of glass fiber meshes coated with PTFE, is set on the stator ring. Agitation in the mixer is carried out by a lifter-turbine impeller which has 6-blade of 10 mm height and 14 mm width under a disk of 50 mm diameter. The impeller position is 51 mm from the bottom of column to the upper surface of impeller disk.

An aqueous solution of I_2-KI is fed to the mixer, rises into the settler through the coalescer and is led to the leveler from the bottom of the settler. A dispersed phase of heptane is started feeding to the mixer after filling the column with the aqueous solution, rises through the coalescer with the aqueous phase and goes out from the top of the column. Iodine in the aqueous phase is extracted into the organic phase in the column, and the concentrations in the outlet aqueous and

organic phases decrease with time and become constant. Since steady state is achieved after flowing ca. 0.0018 m^3 solution (about four times volume of the mixer), aqueous and organic samples are taken from the outlet levelers after flowing ca. 0.005 m^3 solution. Iodine concentrations in the organic phase are determined by a spectrophotometer and those in the aqueous phase by the titration with a solution of sodium thiosulfate. The distribution ratio of iodine, *m*, between aqueous solution and heptane is determined for each experimental run by measuring the iodine concentrations in both phases after equilibrating the outlet organic phase with the outlet aqueous phase. The distribution ratios, which vary with the concentration of iodic ion[43], were between 5 and 8 in the present experiments. For this value of *m*, the mass transfer resistance in aqueous phase is dominant.

In the measurement of mass transfer coefficient within the dispersed phase, a heptane solution of iodine is fed as a dispersed phase and an aqueous solution of sodium thiosulfate as a continuous phase, and the iodine concentrations in the outlet organic phase and the feed solution are measured. The physical properties used in the present study are shown in Table 1, which are almost same as heptane-water system.

Table 1 Physical properties of phases

	dispersed phase	continuous phase
density [kg/m^3]	682	997
viscosity [Pa·s]		8.94×10^{-4}
diffusivity [m^2/s]	3.86×10^{-9}	1.33×10^{-9}
interfacial tension [N/m]	5.06×10^{-2}	

6.2 Results and Discussion

6.2.1 Volumetric over-all mass transfer coefficient

It is assumed that the extraction of iodine proceeds only within the mixer and both the concentrations of continuous and dispersed phases leaving the mixer are equal to those within the mixer (i.e., complete mixing). The volumetric over-all mass transfer coefficient, $K_c a$, based on the continuous phase concentration is obtained by the following equation.

$$K_c a\,(C_{c,out} - C_{c,out}^*)\,V_M = Q_c(C_{c,in} - C_{c,out}) \tag{12}$$

Where C_c is the iodine concentration in aqueous phase, V_M volume of the mixer, Q_c flow rate of aqueous phase and suffixes, out and in, express outlet and inlet, respectively. $C_{c,out}^*$ is the aqueous concentration in equilibrium with the outlet organic phase and given by $C_{c,out}^* = C_{d,out}/m$, where $C_{d,out}$ is the average concentration of outlet organic droplets. The assumption of complete mixing does not mean a uniform concentration of the dispersed phase, but the average concentration of dispersed drops leaving the mixer is equal to that within the mixer. Dispersed drops have various concentrations corresponding to the residence time of the drop in the mixer.

The values of $K_c a$ are shown in Figs.20 and 21 for a constant flow rate of continuous phase and that of dispersed phase, respectively. $K_c a$ increased with the agitation speed, *n*, and the value for $n = 12.1\ s^{-1}$ is about ten times that for $n = 5.7\ s^{-1}$. The effect of dispersed phase flow rate, Q_d, on $K_c a$ in Fig.20 is larger than that of continuous phase flow rate in Fig.21. $K_c a$ increases with the increase in Q_d, while it decreases with the increase in Q_c.

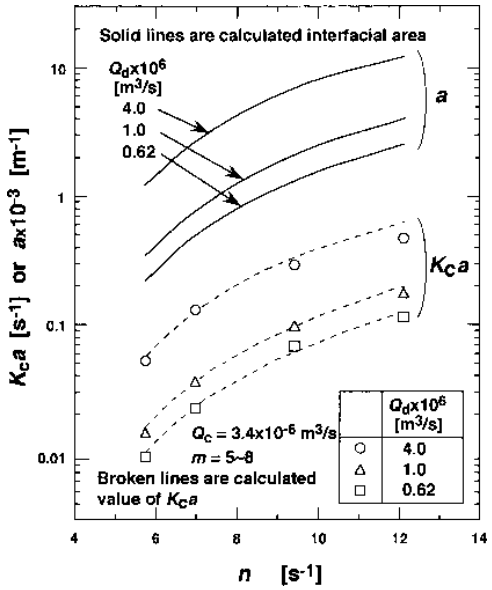

Fig.20 Effect of dispersed phase flow rate on volumetric over-all mass transfer coefficient

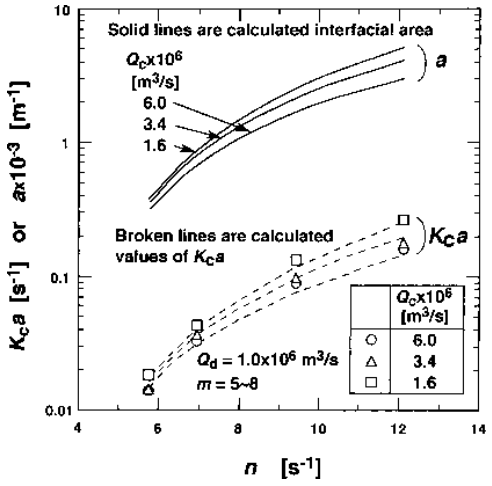

Fig.21 Effect of continuous phase flow rate on volumetric over-all mass transfer coefficient

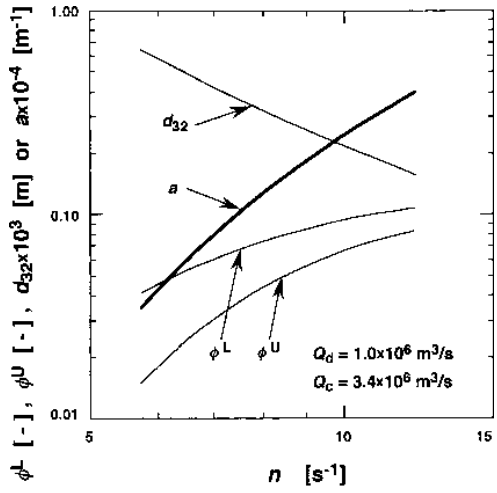

Fig.22 Calculated values of drop size, dispersed phase holdup and specific interfacial area

6.2.2 Interfacial area

To obtain the mass transfer coefficient, specific interfacial area, a, in the mixer must be known, which is given by

$$a = 6\phi / d_{32} \tag{13}$$

where ϕ is dispersed phase holdup in the mixer and d_{32} Sauter mean diameter of dispersed drops. In the present mixer the value of ϕ below the impeller differed from that above the impeller, the value of ϕ could be obtained by averaging ϕ^U and ϕ^L as

$$\phi = (\phi^U V^U + \phi^L V^L) / V_M \tag{14}$$

Where V^L and V^U are volumes below and above the impeller, respectively, and V_M the volume of mixer. The value of ϕ^U is calculated by Eqs.(7) and (8), and ϕ^L by Eqs.(5)–(7). On the other hand, d_{32} is correlated by Eq.(11). The specific interfacial area can be calculated from Eqs.(13) and (14) with the assumption that the values of d_{32} above and below the impeller are same. An example of calculated value of a for the present experimental condition is shown in Fig.22 with ϕ^U, ϕ^L and d_{32}. As the agitation speed increases, values of ϕ^U and ϕ^L increase and d_{32} decreases, i.e., the interfacial area increases largely with the increase in n. The calculated values of a for each experiment are shown in Figs.20 and 21. It increases with n or Q_d and decreases with Q_c. The changes in $K_c a$ are similar to those in a, i.e., the volumetric over-all mass transfer coefficient varies according to the change in interfacial area. The over-all mass transfer coefficient K_c does not change with n, Q_d or Q_c.

6.2.3 Over all mass transfer coefficient

The over-all mass transfer coefficient K_c was obtained by dividing the volumetric coefficient by the interfacial area and shown in Fig.23 as Sh_{Oc} ($=K_c d_{32}/D_c$) to compare with the data for vari-

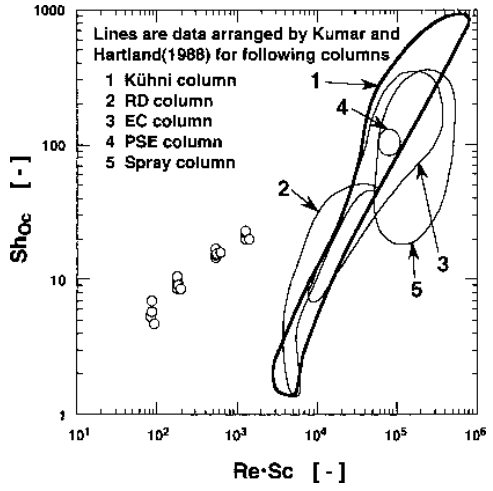

Fig.23 Correlation of Sh_{Oc} against Re·Sc

ous extraction columns given by Kumar and Hartland[44]. The diffusion coefficient of iodine in water was given by Darral and Oldham[45] as in Table 1. Reynolds number, Re, in the abscissa was obtained with the slip velocity (relative velocity) calculated by Eq.(7) with the column cross sectional area and ϕ^{L} instead of A and ϕ^{U} in Eq.(7), respectively.

According to Kumar and Hartland, correlation for several extraction columns, i.e., Kühni column, rotating disc column (RD), enhanced coalescing column (EC) and pulsed sieve extraction column (PSE) are almost same. While, the correlation is apart from the present experimental points. Reynolds number in the present experiments is small due to the small slip velocity because of the small drop diameter. Drop diameters were in the range of 0.15–0.67 mm as shown in Fig.22. With such a small drop diameter, the extraction columns given by lines 1–5 in Fig.23 could not be operated. Since relatively large number of drops circulate within the mixer in the present experiments, the dispersed phase holdup is larger than that in the Kühni column (line 1), and v_s calculated by Eq.(7) are small as 0.0007–0.003 m/s. Because the distribution ratio in the present experiments is large, mass transfer resistance in the continuous phase is dominant and Sh_{Oc} is larger than the theoretical value of $Sh_c = 2$ for the quiescent continuous phase.

6.2.4 Dispersed phase mass transfer coefficient

The volumetric dispersed phase mass transfer coefficient, $k_d a$, was determined by the following equation from the back extraction of iodine in the iodine-heptane solution by the aqueous solution of sodium thiosulfate.

$$k_d a C_{d,out} V_M = Q_d (C_{d,in} - C_{d,out}) \tag{15}$$

Where $C_{d,in}$ is the inlet iodine concentration in heptane. The iodine concentration at the interface was assumed to be zero because of the instantaneous reaction between iodine from the organic phase and sodium thiosulfate in the aqueous phase. The effects of flow rates of dispersed and continuous phases on $k_d a$ are shown in Figs.24 and 25, respectively. The value of $k_d a$ increased

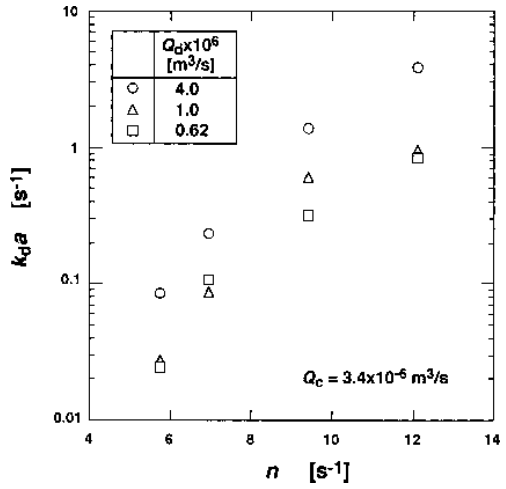

Fig.24 Effect of dispersed phase flow rate on volumetric dispersed phase mass transfer coefficient

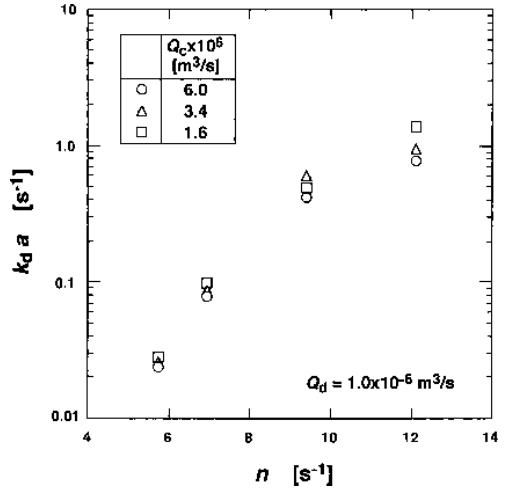

Fig.25 Effect of continuous phase flow rate on volumetric dispersed phase mass transfer coefficient

with the increase in Q_d, while it varied little with the change in Q_c.

By use of the calculated interfacial area, the dispersed phase mass transfer coefficients were obtained from the volumetric mass transfer coefficients in Figs.24 and 25 and shown in Fig.26. The coefficient increased with the agitation speed, but it varied little with the change in Q_d or Q_c.

6.2.5 Dispersed phase mass transfer coefficient based on rigid sphere model

For the present back-extraction, the average concentration, $C_{d,t}$, of iodine in a drop of resi-

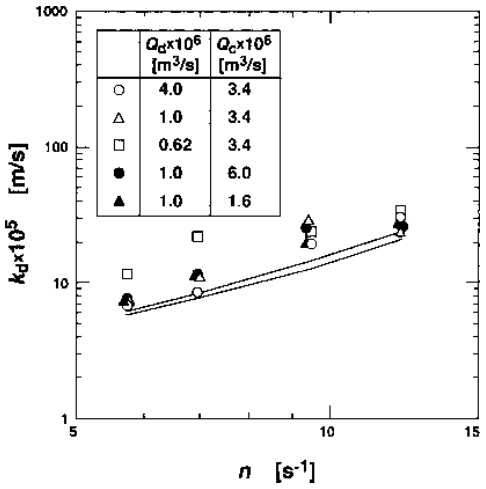

Fig.26 Dispersed phase mass transfer coefficient, lines are calculated form Eq.(19)

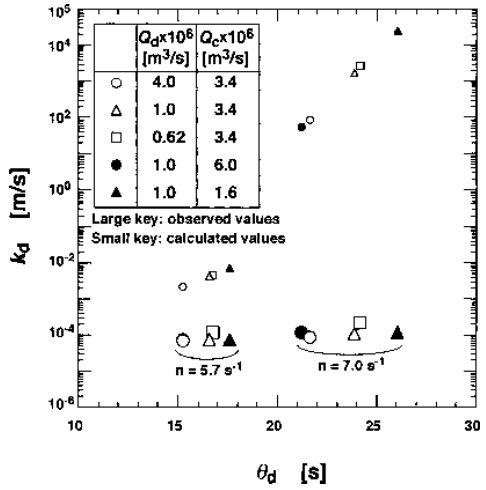

Fig.27 Comparison between k_d calculated for drop of average residence time and observed values

dence time t is given by the diffusion model within a rigid sphere as follows [46].

$$\frac{C_{\mathrm{d,in}} - C_{\mathrm{d,t}}}{C_{\mathrm{d,in}}} = 1 - \frac{6}{\pi^2} \sum_{\mathrm{n}=1}^{\infty} \frac{1}{\mathrm{n}^2} \exp\left(- \frac{4 D_d \mathrm{n}^2 \pi^2 t}{d^2} \right) \tag{16}$$

The value of $C_{\mathrm{d,out}}$ was calculated by use of the average residence time $\theta_{\mathrm{d}} (= V_{\mathrm{M}} \phi / Q_{\mathrm{d}})$ as t in Eq.(16), and k_{d} was determined from Eq.(15).

The calculated values of k_d are larger by several orders than the observed ones as shown in Fig.27. The calculated concentration of outlet drop having the residence time θ_d is very small. There are drops of various residence times, and the concentration of drop increases with the decrease in the residence time. Therefore, the average concentration of outlet drops may differ from the value calculated by the average residence time.

Under an assumption of the complete mixing within the mixer, the residence time distribution is expressed as

Then, the fraction, Y, of iodine back extracted within the mixer is given as

On the other hand, the dispersed phase mass transfer coefficient is derived from Eq.(15) as follows

$$k_d = \frac{Q_d}{aV_M}\frac{C_{d,in}-C_{d,out}}{C_{d,out}} = \frac{d_{32}}{6}\frac{Q_d}{\phi V_M}\frac{YC_{d,in}}{C_{d,out}} = \frac{d_{32}}{6\theta_d}\quad Y$$

The value of k_d calculated by Eq.(19) is shown in Fig.28. In the calculation, Sauter mean diameter d_{32} was used as the drop diameter d in Eq.(16), and the diffusion coefficient of iodine in heptane was estimated with Wilke-Chang correlation by use of the observed value for CO_2 in heptane (Sherwood et. al.[47]) as shown in Table 1. Although k_d decreases with θ_d, the change is very small for $\theta_d > 10$ s. In the present experiments θ_d varied between 15 s and 51 s, and the effect of θ_d on k_d could be negligible.

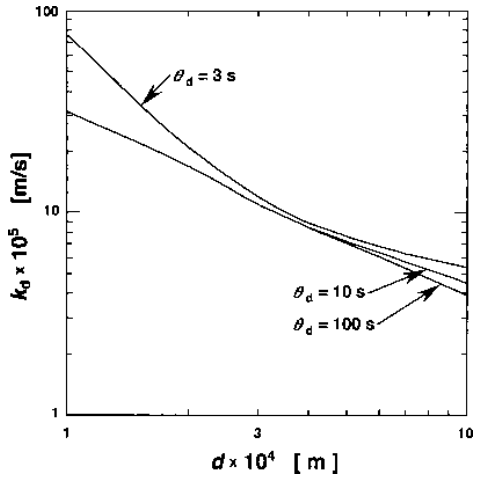

Fig.28 Dispersed phase mass transfer coefficient based on rigid sphere model

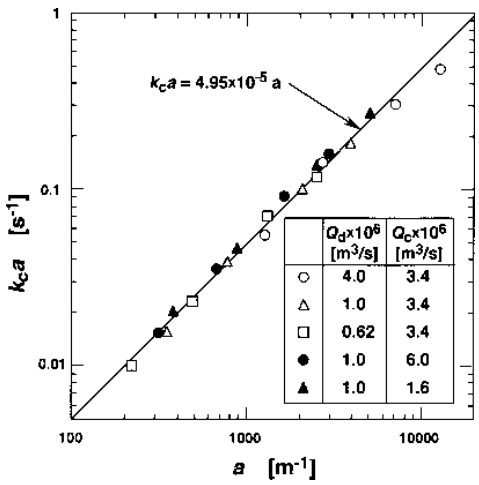

Fig.29 Correlation between volumetric mass transfer coefficient in continuous phase and specific interfacial area

The theoretical values of k_d calculated for the experimental conditions are shown in Fig.26 with two lines as a largest and a smallest values for various flow rates of the dispersed and the continuous phase. The variation of calculated k_d with the flow rates is small and it mainly depends on the change in drop diameter which varies with the average residence time, i.e., the dispersed phase holdup. Though all experimental values are somewhat larger than the theoretical ones, the difference between them is small. It can be concluded that the dispersed phase mass transfer coefficient can be calculated based on the diffusion model within the droplet by taking into account the residence time of the drops.

6.2.6 Continuous phase mass transfer coefficient

According to the addition rule of mass transfer resistance expressed by the volumetric mass transfer coefficients

$$1 / K_c a = (1 / k_c a) + (1 / m k_d a) \tag{20}$$

The volumetric mass transfer coefficients, $k_c a$, in the continuous phase were determined from $K_c a$ in Figs.20 and 21 and $k_d a$ in Fig.24 and 25. As shown in Fig.29, $k_c a$ is proportional to the specific interfacial area, that is, k_c varies little with the agitation speed or the flow rates of dispersed and continuous phases.

The dispersed drops are circulated with the continuous phase below the impeller in the mixer. When the drop diameter is small as in the present experiment, the relative velocity between the drop and the continuous phase may be small, which depends on the gravitation force. Here, we assume that the terminal settling velocity of a rigid sphere having the same diameter and density as the dispersed drop expresses the relative velocity. The terminal velocity, v_t, is given as follows [48].

$$v_t = d^2 \Delta \rho g / 18 \eta \quad \text{for Re} < 1 \tag{21}$$

$$v_t = [\{(A_1^2 + A_2)^{1/2} - A_1\} / 1.1]^2 \quad \text{for Re} < 10^4 \tag{22}$$

where $A_1 = 4.8\,(\eta / \rho_c d)^{1/2}$, $A_2 = 2.54\,(\Delta\rho g d / \rho_c)^{1/2}$

The mass transfer coefficient around a rigid sphere is correlated by Ranz and Marshall[49] as follows.

$$\text{Sh}_c = 2.0 + 0.60\,\text{Re}^{1/2}\text{Sc}^{1/3} \tag{23}$$

The continuous phase mass transfer coefficients, k_c, for the present experiments are determined from values of $k_c a$ and a obtained above, and Sh_c are plotted against $\text{Re}^{1/2}\text{Sc}^{1/3}$ in Fig.30, where Re are calculated with the terminal velocities of drops as mentioned above. In the figure, Eq.(23) is also drawn with a solid line. The present experimental results coincides very well with the correlation of the solid line, that is, the continuous phase mass transfer coefficient can be given by the mass transfer coefficient around a rigid sphere calculated with the terminal settling velocity as the relative velocity between phases. The over-all volumetric mass transfer coefficients $K_c a$ for the conditions as in Figs.20 and 21 are calculated from Eqs. (11), (13), (14), (19), (20) and (23). The calculated values are shown in Figs.20 and 21 by broken lines, which agree very well with the observed values.

The volumetric mass transfer coefficient $k_c a$ of the continuous phase could be calculated from $K_c a$ and $k_d a$ by use of the addition rule of mass transfer resistance. By using the specific interfacial area a estimated from the Sauter mean diameter d_{32} of dispersed drops and the dispersed phase holdup ϕ, the mass transfer coefficients K_c, k_d and k_c could be determined from $K_c a$, $k_d a$ and $k_c a$, respectively. The correlation for K_c in the literature, which could be applied for Kühni column, RDC, EC column and PSE column, could not be applied for the present MS column where the diameter of dispersed drops was smaller by about one order in magnitude than those in above columns. The dispersed phase mass transfer coefficient k_d depended on agitation speed but not on the flow rates of both phases. The value of k_d coincided with the theoretical value based on the

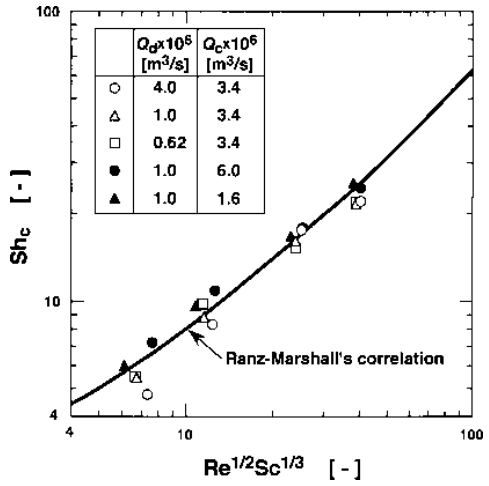

Fig.30 Correlation for continuous phase mass transfer

diffusion within a rigid sphere using the residence time distribution of dispersed drops. The continuous phase mass transfer coefficient k_c did not vary with the agitation speed as well as the flow rates of both phases. The continuous phase mass transfer coefficient could be given by the correlation of mass transfer around a rigid sphere. The terminal settling velocity of a rigid sphere with the same diameter and density as the dispersed drop was used as the relative velocity between the dispersed drop and the continuous phase.

7. Stage Efficiency in MS Column

The stage efficiency is convenient for the calculation of the practical stage number in the multistage counter current extraction column. The efficiency depends on the mass transfer coefficients, the interfacial area, the flow rates and the axial mixing between stages. The stage efficiency of the MS column has been measured with the iodine extraction from aqueous phase into heptane. The effects of the agitation speed, the flow ratio of the dispersed phase to the continuous phase

into five stages of 60 mm in height by stator rings of 31 mm in opening diameter. The top and the bottom stages were used as the settlers, and a 6-blade turbine impeller of 30 mm in diameter was set at the center of each stage for three stages. Time to reach a steady state was about twice of that for the MS column.

7.2 Results and Discussion

7.2.1 Stage efficiency

Liquid-liquid equilibrium for the extraction of iodine from aqueous phase into heptane is given by

$$C_{\mathrm{d}} = mC_{\mathrm{c}} \tag{24}$$

where C_{d} and C_{c} are the iodine concentrations in heptane and aqueous phase, respectively, and m distribution ratio of iodine which is expressed by $m = 36.6/(1 + 748[\mathrm{I}^-])$[43], where $[\mathrm{I}^-]$ is iodic ion concentration in kmol/m^3. Since mutual solubilities between heptane and water are very small, the operating line for the multistage counter-current extraction is expressed by

$$C_{\mathrm{d,p}} - C_{\mathrm{d,in}} = (Q_{\mathrm{c}}/Q_{\mathrm{d}})(C_{\mathrm{c,p+1}} - C_{\mathrm{c,out}}) \tag{25}$$

where Q_{c} is the raffinate phase flow rate, Q_{d} the extract phase flow rate, $C_{\mathrm{d,in}}$ the iodine concentration in organic phase fed to the bottom of the column, and $C_{\mathrm{c,out}}$ the iodine concentration in aqueous phase from the bottom of the column. Stage number is counted from the bottom of the column. The stage efficiency E_{Od} based on the concentration of organic phase is defined as follows.

$$E_{\mathrm{Od}} = (C_{\mathrm{d,p}} - C_{\mathrm{d,p-1}}) / (C_{\mathrm{d,p}}{}^* - C_{\mathrm{d,p-1}}) \tag{26}$$

Where $C_{\mathrm{d,p}}{}^*$ (= $mC_{\mathrm{c,p}}$) is the organic phase concentration in equilibrium with the aqueous phase of p-th stage. The equilibrium line and the operating line given by Eqs.(24) and (25), respectively, are straight lines on C_{d}–C_{c} diagram as shown in Fig.31. Under an assumption that the stage efficiency does not vary with the stage number, the points ($C_{\mathrm{c,\,out}}$, $C_{\mathrm{d,\,1}}$), ($C_{\mathrm{c,\,2}}$, $C_{\mathrm{d,\,2}}$), · · · , ($C_{\mathrm{c,\,p}}$, $C_{\mathrm{d,\,p}}$), · · · ,

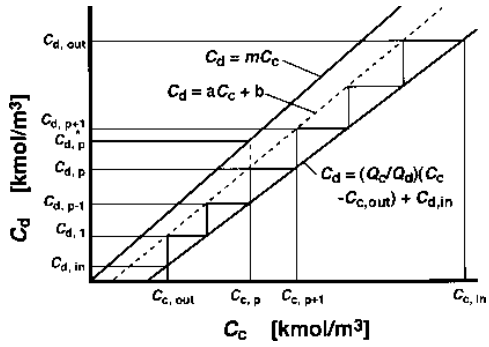

Fig.31 Diagram to determine stage efficiency

($C_{c,\,p}$, $C_{d,\,out}$), which represent the concentrations of the dispersed and the continuous phases leaving the stage, are on a straight line as shown by $C_d = aC_c + b$ in Fig.31, and the following relation can be obtained.

$$C_{d,p} - C_{d,p-1} = (Q_c / Q_d)(C_{c,p+1} - C_{c,p}) \tag{27}$$

$$C_{d,p+1} - C_{d,p} = a(C_{c,p+1} - C_{c,p}) \tag{28}$$

From these equations

$$C_{d,p+1} - C_{d,p} = r\,(C_{d,p} - C_{d,p-1}) \tag{29}$$

where $r = a/(Q_c/Q_d)$. The series $\{C_{d,p} - C_{d,p-1}\}$ is a geometric progression, and the summation of the series is

$$\sum \{C_{d,p} - C_{d,p-1}\}$$

$$= C_{d,out} - C_{d,in} = (C_{d,1} - C_{d,in})(1 + r + r^2 + \cdots + r^{P-1}) \tag{30}$$

From the definition of the stage efficiency,

$$E_{Od} = \frac{C_{d,p} - C_{d,p-1}}{C^*_{d,p} - C_{d,p-1}} = \frac{(aC_{c,p}+b) - \{(Q_c/Q_d)(C_{c,p} - C_{c,out}) + C_{d,in}\}}{mC_{c,p} - \{(Q_c/Q_d)(C_{c,p} - C_{c,out}) + C_{d,in}\}} \tag{31}$$

This equation is rearranged as follows.

$$\{a - mE_{Od} - (1 - E_{Od})(Q_c / Q_d)\}C_{c,p} + b - (1 - E_{Od})$$

$$\times \{C_{d,in} - (Q_c / Q_d)\,C_{c,\,out}\} = 0 \tag{32}$$

To satisfy Eq.(32) for any value of $C_{c,p.}$

$$a = mE_{Od} + (1 - E_{Od})(Q_c/Q_d),$$

$$b = (1 - E_{Od})\,\{C_{d,in} - (Q_c/Q_d)\,C_{c,out}\} \tag{33}$$

By substituting $C_{d,\,1} - C_{d,\,in} = E_{Od}\,(C_{d,\,1}{}^* - C_{d,\,in}) = E_{Od}(mC_{c,\,out} - C_{d,\,in})$ to Eq.(30),

$$E_{Od}\,(mC_{c,\,out} - C_{d,\,in})\,(1 + r + r^2 + \cdots + r^{P-1}) - (C_{d,\,out} - C_{d,\,in}) = 0 \tag{34}$$

where

$$r = a\,(Q_c / Q_d) = E_{Od}\{m / (Q_c / Q_d) - 1\} + 1 \tag{35}$$

The ratio of flow rate is given by $Q_c/Q_d = (C_{d,out} - C_{d,in})(C_{c,in} - C_{c,out})$ from the mass balance of the column. The value of E_{Od} can be determined from Eqs.(34) and (35) with the measured values of $C_{c,,\,in}$, $C_{c,,\,out}$, $C_{d,\,in}$, $C_{d,\,out}$ and m.

7.2.2 Effects of agitation speed, flow rates and distribution ratio on stage efficiency

Stage efficiencies E_{Od} of MS column and the MIXCO column are shown in Fig.32 against the agitation speed n for the distribution ratio m = 6.0 and flow ratio Q_c/Q_d = 4. E_{Od} of MS column increased monotonously with the increase in n and high stage efficiency could be obtained at a strong agitation in the present experimental condition. While E_{Od} of the MIXCO column stops increasing for large value of n, and the value is smaller than that of the MS column in spite of the fact that the holdup of dispersed phase (i.e., the interfacial area) of the MIXCO column is larger than that of MS column. The stage efficiency of the MIXCO column may be affected by the axial mixing between stages. Since the axial mixing increased with the agitation speed, the difference in E_{Od} between two columns became large with n. The MS column may be a high performance extraction column, which can achieve large stage efficiency as well as a large throughput and a stable operation at a vigorous agitation. However, if the agitation speed is continued to increase, a large part of dispersed drops will pass through the coalescer without coalescing and be accompanied by the continuous phase, the decrease in the stage efficiency follows. Though smaller drops can be coalesced with the coalescer of smaller mesh pitch, the pressure drop by the coalescer increases with the decrease in mesh pitch, which decreases the throughput[17].

The effect of throughput on the stage efficiency is given in Fig.33 for a given Q_c/Q_d and m. Here, U_O and U_W are superficial velocities of the dispersed and the continuous phases respectively, and $U_O + U_W = 1.33 \times 10^{-3}$ m/s corresponds to $Q_d + Q_c = 3.75 \times 10^{-6}$ m^3/s for the present column. E_{Od} varied little with the total throughput $U_O + U_W$. The holdup of dispersed phase increases with the increase in U_O and decrease with the increase in U_W, and the effect of U_O is larger than that of U_W[22], i.e., the holdup may increase by doubling $U_O + U_W$ under a constant Q_c/Q_d. While the resi-

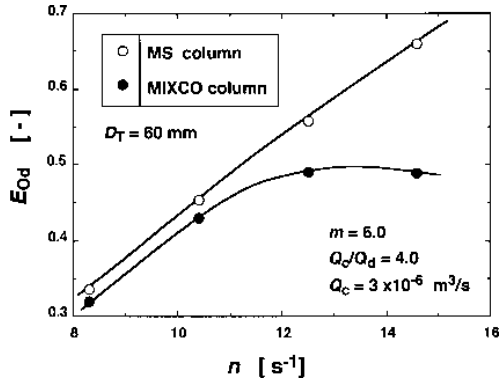

Fig 32 Comparison of stage efficiencies between MS column and MIXCO column

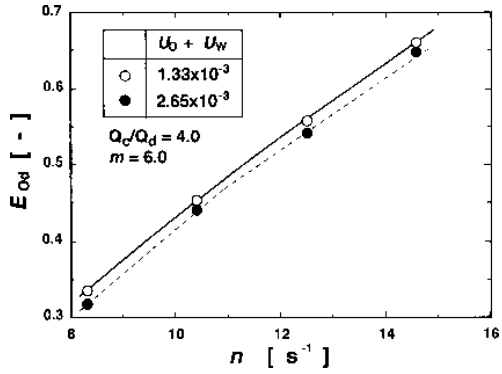

Fig.33 Effect of throughput on stage efficiency

dence time of dispersed phase decreases with the increase in U_W, and the size of dispersed drop increases with the decrease in the residence time[21]. As the effect of the flow rate on the stage efficiency, the contribution of the holdup is positive and that of the residence time is negative, because the interfacial area is proportional to the holdup and inversely proportional to the drop size. The former may be compensated by the latter in case of Fig.33. On the other hand, E_{Od} for a given m increased with the flow ratio Q_c/Q_d, and that for a given Q_c/Q_d decreased with the distribution ratio m as shown in Figs.34 and 35.

When the stage efficiency E_{Oc} defined by the following equation with the concentration of continuous phase is used, the dependency of the stage efficiency on m and Q_c/Q_d may be different from the above results.

$$E_{Oc} = (C_{c,p} - C_{c,p+1}) / (C^*_{c,p} - C_{c,p+1}) \tag{36}$$

Where $C^*_{c,p} = C_{d,p} / m$. In the same way as for E_{Od}, the following equation can be derived.

$$(E_{Oc} r / m)(mC_{c,out} - C_{d,in})(1 + r + r^2 + \cdots + r^{P-1}) - (C_{c,in} - C_{d,out}) = 0 \tag{37}$$

Where $r = 1/\{E_{Oc}(Q_c/Q_d)/m + 1 - E_{Oc}\}$. In Fig.35, E_{Oc} for the same data used to calculate E_{Od} are also plotted against m. E_{Oc} increases with the increase in m, in contrast to the change of E_{Od}. The value of E_{Oc} is larger than E_{Od} for $m > Q_c/Q_d$ and the reverse is also true. The change of E_{Oc} is large for $m < Q_c/Q_d$, while that of E_{Od} is large for $m > Q_c/Q_d$.

7.2.3 Estimation of stage efficiency

Under the assumption that mass transfer occurs only within the mixer and the concentrations $C_{c,p}$ and $C_{d,p}$ of the outlets from p-th stage are equal to those in the mixer, i.e., complete mixing within the mixer, the volumetric over-all mass transfer coefficient, $K_c a$, based on the continuous phase concentration is given as

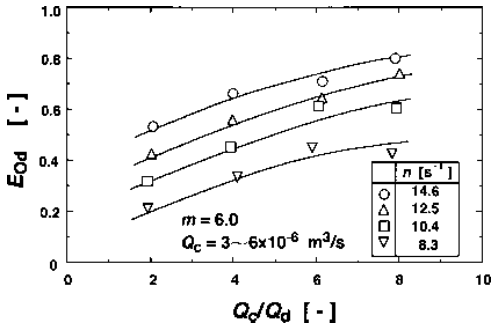

Fig.34 Effect of flow ratio on stage efficiency

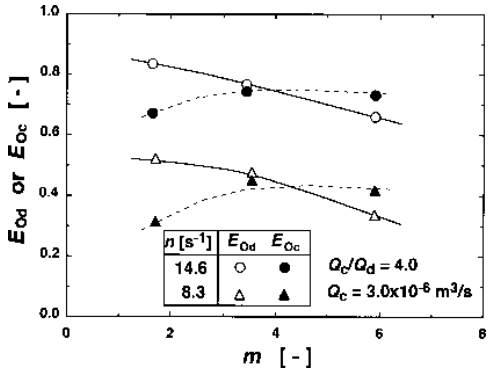

Fig.35 Effect of distribution ratio on stage efficiency

$$K_c a V_M (C_{c,p} - C_{c,p}^*) = Q_c (C_{c,p-1} - C_{c,p}) \tag{38}$$

where V_M is volume of the mixer. Equation (38) is rearranged as

$$K_c a V_M / Q_c = (C_{c,p-1} - C_{c,p}) / (C_{c,p} - C_{c,p}^*) \tag{39}$$

From Eqs.(36) and (39), following relation between the stage efficiency and the volumetric mass transfer coefficient is derived.

$$E_{Oc} = (K_c a V_M / Q_c) / \{1 + (K_c a V_M / Q_c)\} \tag{40}$$

In the same way, the stage efficiency, E_{Od}, based on the dispersed phase concentration is expressed as follows.

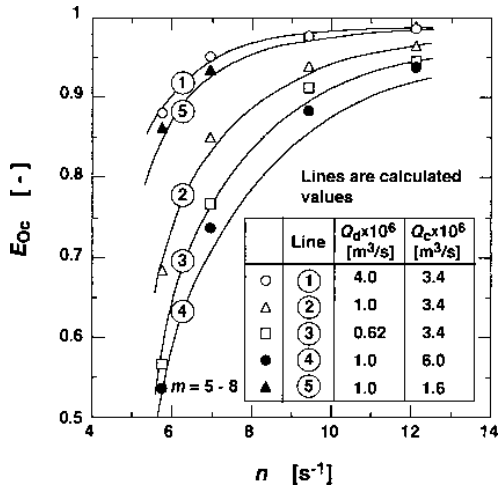

Fig.36 Comparison of experimental stage efficiencies with calculated ones

$$E_{Od} = (K_d a V_M / Q_d) / \{1 + (K_d a V_M / Q_d)\} \tag{41}$$

Where $C_{d,p}$* is the dispersed phase concentration in equilibrium with $C_{c,p}$, $K_d a$ the volumetric over-all mass transfer coefficient based on dispersed phase concentration (= (Q_d / V_M) $(C_{d,p} - C_{d,p+1})$/ $(C_{d,p}^* - C_{d,p})$). The stage efficiency can be determined by Eq.(40) or (41) if the volumetric over-all mass transfer coefficient is estimated.

By using the extraction data with a single stage MS column with which the values of $K_c a$ in Figs.20 and 21 were obtained, the stage efficiency E_{Oc} is calculated by Eq.(36) and shown in Fig.36. The efficiency increases with the agitation speed in the same way as in Fig.32, and it increases with the increase in the dispersed phase flow rate and decreases with the increase in the continuous phase flow rate. For the experimental conditions of Fig.36, the stage efficiency is calculated from Eq.(40) with $K_c a$. The over-all volumetric mass transfer coefficient $K_c a$ is calculated from Eq.(20) with a, k_c and k_d. The interfacial area a is calculated from Eq.(13) with ϕ and d_{32}. The dispersed phase holdup ϕ is calculated from Eq.(14) with ϕ^U and ϕ^L. The holdup ϕ^U above the impeller in the mixer is calculated from Eqs.(7) and (8), and ϕ^L below the impeller from Eqs.(5)–(7). The drop size d_{32} is obtained from the correlation of Eq.(11). The continuous phase mass transfer coefficient k_c is calculated from Eq.(23) with the terminal settling velocity v_t given by Eqs.(21) and (22). The dispersed phase mass transfer coefficient is calculated from Eq.(19) using Eqs.(16)–(18). The calculated results are shown with solid lines in Fig.36. They agree well with the experimental results for any flow rates of both phases. This indicates that the stage efficiency can be estimated rationally for the MS column.

To clarify the effects of flow rates on E_{Oc} or E_{Od}, the stage efficiencies were calculated for various flow rates by use of the same physical properties and the same column geometry as used in Fig.36. Figure 37 show the effects of flow rates on E_{Oc} or E_{Od}. The calculated value of E_{Oc} increases with the increase in Q_d, while E_{Od} decreases largely with the increase in Q_d (solid lines). This behavior can be explicable in terms of the change in interfacial area, a, because the mass transfer coefficients of both phases vary little with the change of flow rate as mentioned above. When the value of Q_d increases at a constant Q_c, the dispersed phase hold-up increases monoto-

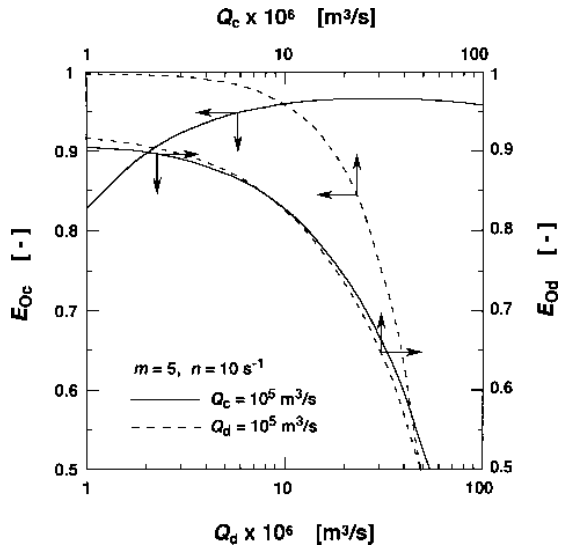

Fig.37 Calculated results for effects of flow rates on stage efficiencies

nously and the drop diameter also increases due to the decrease in the residence time given by $V^L\phi^L/Q_d$. Then the value of a given by $6\phi/d_{32}$ increases for small Q_d and decreases slightly for large Q_d because the drop diameter effect becomes more predominant than the hold-up one. Then the value of E_{Oc} increases with Q_d for small Q_d but slightly decreases for large Q_d. On the other hand, $K_d a V_M/Q_d$ in Eq.(41) decreases with increase in Q_d, then E_{Od} decreases with Q_d as shown in Fig.37. When the continuous phase flow rate increases under constant Q_d, the dispersed phase hold-up decreases and the drop diameter increases, i.e., the value of a decreases with both effects. Since the value of $K_c a V_M/Q_c$ in Eq.(40) decreases with increase in Q_c due to both effects of decreasing a and increasing Q_c, the value of E_{Oc} decreases rapidly with the increase in Q_c as shown by the broken line in Fig.37. The change in E_{Od} with the increase in Q_c in Fig.37 is moderate because $K_d a V_M/Q_d$ in Eq.(41) decreases only by the decrease in a. The experimental values of E_{Od} shown in Fig.34, which were obtained with the small column, have the same tendency as the above description, that is, E_{Od} decreases with Q_d.

Figure 38 shows the calculated effect of the distribution ratio on E_{Oc} and E_{Od} for constant flow rates of $Q_c = Q_d = 10^{-5}$ m^3/s. The value E_{Oc} for a constant agitation speed increases with the increase in m, for $K_c a V_M/Q_c$ in Eq.(40) increases with K_c which increases with the increase in m as given by Eq.(20). The values of E_{Od} decrease with the increase in m, for K_d decreases with m. In case of n = 6 s^{-1} where the value of k_c is nearly equal to k_d, E_{Oc} and E_{Od} in Fig.38 are symmetric each other. However, in case of n = 12 s^{-1}, variation of E_{Oc} is smaller than that of E_{Od} because k_d is larger by several times than k_c. The same effects of m on E_{Oc} and E_{Od} are seen in the experimental results shown in Fig.35.

The stage efficiency of the MS column increased monotonously with the increase in agitation speed. Since stable operation is possible at a high agitation speed with this extraction column, both large stage efficiency and a large throughput, which is desirable for the counter-current extraction column, can be achieved. It is confirmed that the stage efficiency can be estimated rationally by use of the interfacial area and the mass transfer coefficients of the continuous and dis-

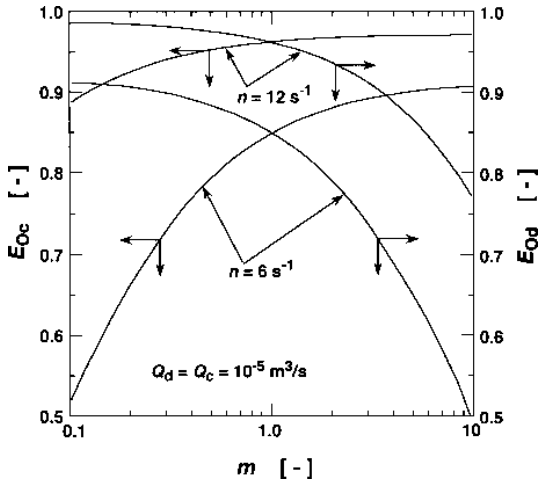

Fig.38 Calculated results for effects of distribution ratio on stage efficiencies

persed phases. The interfacial area is determined with the dispersed phase holdup and the drop size and the mass transfer coefficients in both phases with a rigid sphere model. The calculated stage efficiency E_{Od} based on the dispersed phase concentration increased with the flow ratio Q_c/Q_d of the continuous phase to the dispersed phase. The calculated value of E_{Od} decreases with the increase in m, while E_{Oc} based on the continuous phase concentration increases with m. These tendencies were also observed in the experimental results.

8. Extraction of Copper by MS Extraction Column

Solvent extraction is useful for the removal of heavy metals from wastewater. An effective removal of metal from a dilute solution can be achieved by multistage counter-current extraction. We have proposed a multistage mixer-settler extraction column (MS column) which realizes a large throughput[18] and a high stage efficiency[19] simultaneously under a strong agitation. Copper, one of hazardous materials contained in the wastewater from various electroplating, mines and metallurgy, chemicals, electronic etc. industries[50] must be prevented from being discharged into the environment. Heavy metal in a dilute solution just as a rinse water is difficult to remove, and the separation technique of high efficiency is necessary.

Copper was extracted from a dilute solution through a five-stage MS column, and the extraction rate of copper by LIX84I was measured within a flat interface stirred vessel (FISV)[51]. The simulation for the multi-stage counter-current extraction, where both the mass transfer and the extractive reaction are taken into account, are discussed by use of the specific interfacial area determined from the dispersed phase holdup and the dispersed drop size, mass transfer coefficients in the continuous and the dispersed phases, and the extractive reaction rate at the interface. The simulated results are compared with the observed ones, and the effects of stage number and flow rates of both phases on the removal of copper are estimated by the simulation.

8.1 Experimental

The MS column used for copper extraction is shown schematically in Fig.2. The column was made of acrylic resin pipe of 100 mm inner diameter and has five stages and a drop coalescer at the bottom of the column. Each stage consists of a mixer of 60 mm height and a settler of 40 mm height. A three-dimensional drop coalescer of 12 mm height made of glass fiber mesh coated with PTFE is set on a stator ring of 50 mm opening diameter between the mixer and the settler. A lifter-turbine impeller which has six blades under a disk of 50 mm diameter carries out agitation in the mixer.

The feed solution was an aqueous solution of 0.15 mol/m^3 copper(II) chloride with the pH adjusted to 2.6 by the addition of hydrochloric acid. Diluent was Shellsol 71 (Shell Chemicals Co., Ltd.) and the copper extractant, LIX84I (Henkel Co.), was dissolved in the diluent. The feed solution is fed into the mixer of top stage and contacted with the organic solution. Both the aqueous and the organic solutions rise together through the drop coalescer and separated into each phase within the settler. The aqueous solution goes down into the mixer of lower stage through the downspout, and finally is led to the outlet leveler from the bottom of the column. The organic solution fed to the bottom of the column flows into the bottom stage mixer through the riser tube then rises into the settler with the aqueous solution. After separation from the aqueous phase within the settler, the organic solution rises into upper stage and finally is led to the outlet leveler from the top of the column. The flow rates of the aqueous and the organic solutions were 3.3×10^{-6} and 0.6×10^{-6} m^3/s, respectively. The organic solution was fed after filling the column with the aqueous solution. When the aqueous volume fed to the column exceeded four times of the column volume, the outlet copper concentration became constant (i.e., steady state). The steady state copper concentration in the outlet solution was determined by an atomic absorption spectrophotometer (Shimazu Co., type AA-6400F).

The extraction rates of copper by LIX84I were measured by a FISV. The vessel has 55 mm inside diameter and 200 cm^3 in volume with four baffles and two paddle impellers of 24 mm diameter at height of 12 mm and 35 mm from the bottom of the vessel. The organic solution of 5×10^{-5} m^3 was laid on the aqueous solution of 5×10^{-5} m^3, and both phases were stirred at 2 s^{-1}. The extraction rate of copper was determined from the concentration change in the aqueous phase. Mass transfer coefficients in the organic and the aqueous phases were measured by the iodine transfer from heptane solution of iodine into $Na_2S_2O_3$ aqueous solution and that from I_2-KI aqueous solution into heptane, respectively. These measurements with the stirred vessel were carried out within the water bath of 298 ± 0.5 K.

8.2 Results and Discussion

8.2.1 Copper extraction with MS column

Concentration ratios X (= $C_{A,out}/C_{A,in}$) of copper in the outlet aqueous solution to that in the inlet solution are shown in Fig.39 against agitation speed n. The ratio is reduced largely by changing the extractant concentration $C_{RH,in}$ from 1.78 to 8.78 mol/m^3. For $C_{RH,in}$ = 8.78 mol/m^3 and n = 10 s^{-1}, the value of X is 0.002, which indicates that the effective removal of copper from a dilute aqueous solution is achieved by the multi-stage counter-current extraction.

8.2.2 Mass transfer coefficients in FISV

The extractive reaction between copper ion and LIX84I may proceed at the interface, since copper ion does not dissolve into the organic phase and LIX84I can hardly dissolve into the aqueous phase. It is necessary to estimate the interfacial concentrations by the use of the mass transfer coefficients to assess the effects of the reactants on the interfacial extractive reaction rate at the

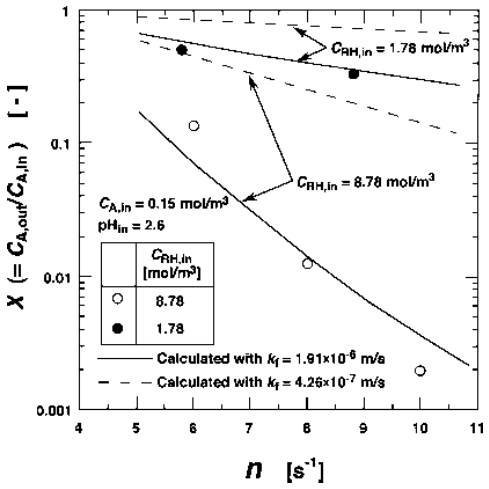

Fig.39 Extraction of copper with a five-stage mixer-settler extraction column

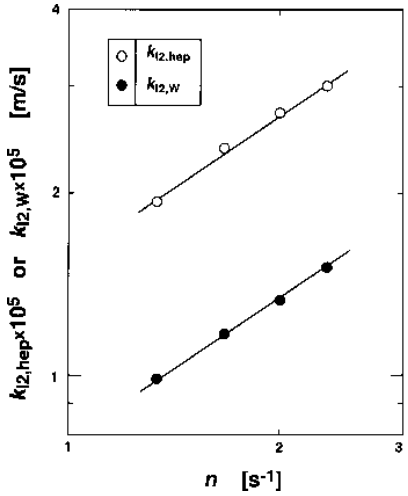

Fig.40 Mass transfer coefficient of iodine transfer within heptane or aqueous solution in FISV

interface. The mass transfer coefficient, $k_{I2,hep}$, in the organic phase was measured by the iodine transfer from heptane into $Na_2S_2O_3$ aqueous solution and shown in Fig.40. It was correlated as follows.

$$k_{12,\mathrm{hep}} = 1.53 \times 10^{-5} n^{0.8} \tag{42}$$

On the other hand, the mass transfer coefficient, $k_{I2,W}$, in the aqueous phase is determined by use of the additive rule of mass transfer resistance from $k_{I2,hep}$ and the over-all mass transfer coefficient, $K_{I2,W}$, measured by the iodine transfer from I_2-KI aqueous solution into heptane. The coefficients $k_{I2,W}$ are also shown in Fig.40 and given by

$$k_{12,W} = 7.9 \times 10^{-5} n^{0.8} \tag{43}$$

The mass transfer coefficient, $k_{RH,O}$, of LIX84I in Shellsol71 is estimated from $k_{I2,hep}$ by the use of the correlation between the mass transfer coefficient and the diffusion coefficient given by Asai et al.[52], where the diffusion coefficients are obtained from Sherwood and Pigford [47].

$$k_{RH,O} = k_{RH,ker} = \left(D_{RH,ker} / D_{I2,hep} \right)^{2/3} k_{I2,hep}$$
$$= \left\{ \left(\frac{D_{RH,ker}}{D_{I2,ker}} \right) \left(\frac{D_{I2,ker}}{D_{I2,hep}} \right) \right\}^{2/3} k_{I2,hep} = \left\{ \left(\frac{V_{I2}}{V_{RH}} \right)^{0.6} \left(\frac{D_{CO2,ker}}{D_{CO2,hep}} \right) \right\}^{2/3} k_{I2,hep} \tag{44}$$

Where V is molar volume at normal boiling point and the subscript, ker, expresses kerosene. Shellsol71 is regarded as the same as kerosene. In the same way, the mass transfer coefficients, $k_{A,W}$, of Cu^{2+} and $k_{H,W}$, of H^+ in the aqueous phase are determined as follows.

$$k_{A,W} = \left(D_{Cu,W} / D_{I2,W} \right)^{2/3} k_{I2,W} \tag{45}$$

$$k_{H,W} = \left(D_{H,W} / D_{I2,W} \right)^{2/3} k_{I2,W} \tag{46}$$

The diffusion coefficients of ions are calculated based on the Vinograd-McBain's equation[53], and the value of $D_{I2,W}$ given by Darrall and Oldham[45] is used.

8.2.3 Copper extraction rate in FISV

Extraction rates, N_A, of copper across the flat interface in the FISV were determined from the change in copper concentration of aqueous phase. Interfacial concentrations were obtained by the following equations.

$$C_{A,i} = C_{A,b} - N_A / k_{A,W} \tag{47}$$

$$C_{H,i} = C_{H,b} + 2N_A / k_{H,W} \tag{48}$$

$$C_{RH,i} = C_{RH,b} - 2N_A / k_{RH,O} \tag{49}$$

Where suffix i and b express interface and bulk of solutions, respectively. Here, it is assumed that $C_{RH,i}$ is independent of the diffusion of complex (CuR_2) in the organic phase. Equations(48) and (49) are derived on the basis of the following extractive reaction.

$$Cu^{2+} + 2RH \rightarrow CuR_2 + 2H^+ \tag{50}$$

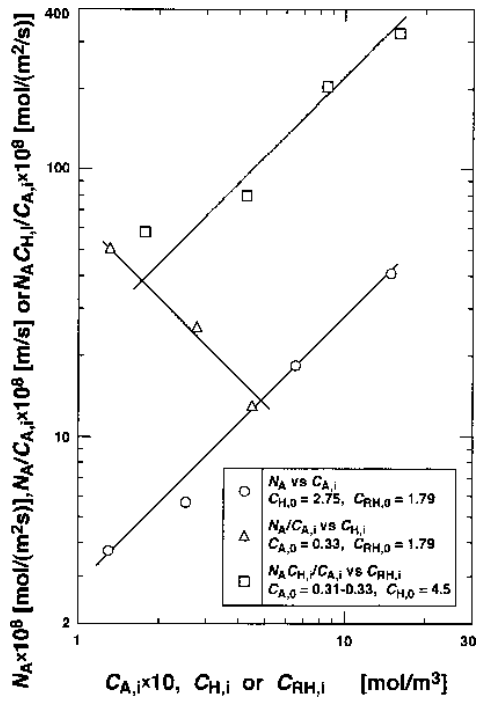

Fig.41 Effects of concentrations of copper, hydrogen ion and LIX84I on extraction rate of copper

Given the interfacial concentrations, the effects of these species on the extraction rate of copper are shown in Fig.41. The apparent extraction rate of copper by hydroxyoxime was given by Komasawa et al.[54] as follows:

$$N_A = k_f C_A C_{RH} / C_H \tag{51}$$

The backward extraction rate is neglected in Eq.(51). The extraction rate is generally given by forward and backward reactions, the backward reaction rate for the present case, however, decreases with the increase in pH value and is very small for pH > 2 (Takahashi and Takeuchi[55]). Since the main component of LIX84I is also hydroxyoxime, the extraction rate of copper in the present case may be expressed by Eq.(51), and the reaction rate constant k_f is determined as 4.26×10^{-7} m/s.

8.2.4 Calculation of copper extraction within MS column

We aim to calculate the outlet concentration of copper, $C_{A,out}$, given the inlet concentrations of copper, $C_{A,in}$, hydrogen ion, $C_{H,in}$, extractant, $C_{RH,in}$, the aqueous phase flow rates, Q_c, the organic phase flow rate, Q_d, the agitation speed, n, and the number of stages, P.

Schematic diagram for the calculation is shown in Fig.42. A stage is counted from the bottom toward the top of the column. The value of $C_{A,out}$, which is equal to $C_{A,1}$ under the assumption of complete mixing within the stage, is assumed, and the calculation is carried out stage to stage from the bottom toward the top of the column. If the calculated value, $C_{A,P+1}$ is not equal to $C_{A,in}$, the

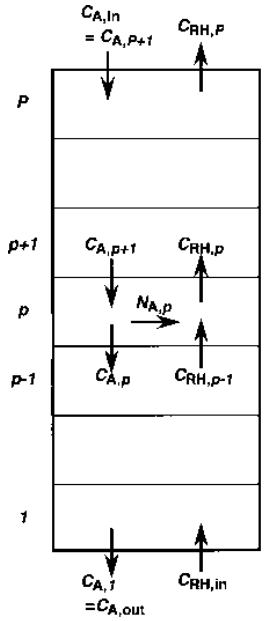

Fig.42 Diagram for calculation of multi-stage counter-current extraction

calculation is repeated with another assumed value of $C_{A,out}$ until $C_{A,P+1} = C_{A,in}$, and the value $C_{A,out}$ is determined.

For the p-th stage, $C_{A,p+1}$, $C_{H,p+1}$ and $C_{RH,p}$ are given by the following equations, respectively.

$$C_{A,p+1} = C_{A,p} + N_{A,p} a V_M / Q_c \tag{52}$$

$$C_{H,p+1} = C_{H,p} - 2N_{A,p} a V_M / Q_c \tag{53}$$

$$C_{RH,p} = C_{RH,p-1} - 2N_{A,p} a V_M / Q_d \tag{54}$$

Where $N_{A,p}$ is the extraction rate in p-th stage, a is the specific interfacial area in the mixer and V_M is the volume of the mixer. When $C_{A,p}$, $C_{H,p}$ and $C_{RH,p-1}$ are known, $C_{RH,p}$ is given by Eq.(54) and the interfacial concentrations $C_{A,p,i}$, $C_{H,p,i}$ and $C_{RH,p,i}$ are obtained from the same equations as Eqs.(47)–(49). By substituting these interfacial concentrations into Eq.(51), the following 2nd order equation of $N_{A,p}$ is obtained.

$$AN_{A,p}^2 + BN_{A,p} + C = 0 \tag{55}$$

Where

$$A = k_f \left(\frac{1}{k_{A,c}}\right)\left\{\left(\frac{2aV_M}{Q_d}\right) + \left(\frac{2}{k_{RH,d}}\right)\right\} - \left(\frac{2}{k_{H,c}}\right)$$

$$B = -k_f\left[C_{A,p}\left\{\left(\frac{2aV_M}{Q_d}\right)+\left(\frac{2}{k_{RH,d}}\right)\right\}+\left(\frac{C_{RH,p-1}}{k_{A,c}}\right)\right]-C_{H,p}$$

$$C = k_f C_{A,p} C_{RH,p-1}$$

where $k_{A,c}$ and $k_{H,c}$ are the mass transfer coefficient of copper and hydrogen ion in the continuous phase, respectively, and $k_{RH,d}$ is the mass transfer coefficient of extractant in the dispersed phase. The value of $N_{A,p}$ is determined from Eq.(55), and $C_{A,p+1}$, $C_{H,p+1}$ and $C_{RH,p}$ are determined from Eqs.(52)–(54).

8.2.5 Specific interfacial area

The specific interfacial area, a (= $6\phi/d_{32}$), is determined from the Sauter mean diameter, d_{32}, of the dispersed drops and the holdup, ϕ, of dispersed phase in the mixer. The value of d_{32} in the MS column was measured by Takahashi and Takeuchi[21] for tributylphosphate (TBP)-heptane-water system, and given by Eq.(11). The interfacial tension, γ, which appeared in Eq.(11), was measured for the present system by the drop volume method and shown in Fig.43.

The dispersed phase holdup, ϕ^U, above the impeller in the MS column differed largely from ϕ^L below the impeller[22]. Since agitation above the lifter-turbine impeller is mild, ϕ^U can be expressed by Eq.(7) in term of the slip velocity, v_s, between two phases rising concurrently around the impeller. By using v_s measured for TBP-heptane-water system[22], the ratios of v_s to the terminal settling velocity, v_t, are plotted against ϕ^L in Fig.44. The value of v_t is calculated by Eqs.(21) and (22). The value of v_s/v_t for TBP free heptane is independent of ϕ^L and a simple relation was obtained.

$$v_S = 0.21 v_t \tag{56}$$

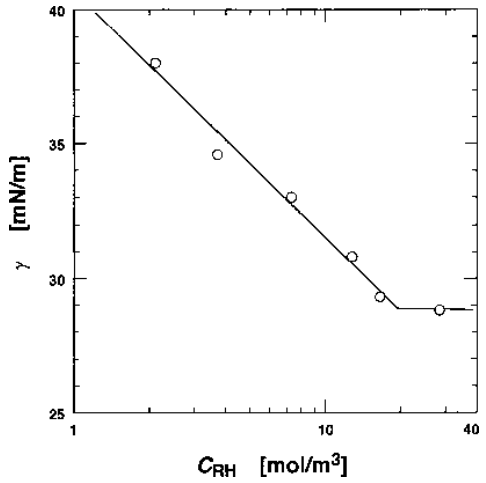

Fig.43 Interfacial tension of LIX84I-heptane-water system

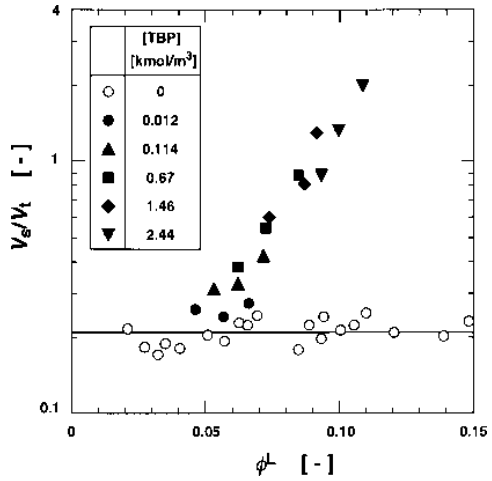

Fig.44 Ratio of slip velocity to terminal settling velocity for TBP-heptane-water system

On the other hand, v_s/v_t for TBP-heptane solution increased with the increase in ϕ^L, and exceeded unity for large concentrations of TBP. Since v_s can not exceed v_t, the increase in v_s/v_t might result from the application of Eq.(11) to TBP-heptane solution. The drop size in the mixer may increase with the dispersed phase holdup in the same way as in the stirred vessel[56]. The effect of dispersed phase holdup on the drop size depends on the drop coalescence in the mixer. The coalescence behavior may vary with the materials consisting two-phase system as well as the existence of mass transfer between phases (Komasawa and Ingham[5]). Equation (11) was derived from the experiments with small holdup of dispersed phase, where the coalescence of drops could be neglected. The actual drop size for TBP solution might be larger than that calculated from Eq.(11) because of the drop coalescence. If the drop size is estimated correctly, v_s may be determined from Eq.(56). For the present extraction system, it is assumed that the coalescence of drop is negligible, and ϕ^U is determined from Eq.(7) by use of Eq.(56).

The holdup ϕ^L below the impeller can be determined from the assumption that the dispersed phase transfers from below to above the impeller by two mechanisms. One is the transfer by mixing due to the difference between ϕ^L and ϕ^U and the other is the transfer by carriage of total flow (Takahashi and Takeuchi[22]). The value of ϕ^L is calculated by Eqs.(5)–(7) given Q_d and Q_c by the use of ϕ^U determined above. In practical calculations, d_{32} can be calculated by the trial and error method with an assumed value of θ_d, where θ_d is determined with ϕ^L obtained by use of d_{32}. The calculation is repeated until the assumed value of θ_d coincides with the calculated one. The specific interfacial area was determined with the average holdup obtained from ϕ^L and ϕ^U by weighting the volumes below and above the impeller.

8.2.6 Mass transfer coefficients within MS column

It was shown by Nii et al.[42] that the mass transfer coefficients in the dispersed and the continuous phases within the MS column can be determined on the basis of mass transfer within and around a rigid sphere, because the dispersed drop is very small (< 1 mm). The dispersed phase mass transfer coefficient, $k_{RH,d}$, for the extractant is calculated by Eqs.(16)–(19). The mass transfer coefficients, $k_{A,c}$ and $k_{H,c}$, of copper and hydrogen ion in the continuous phase are determined

from Eqs.(21)–(23).

The outlet concentration $C_{A,out}$ from the extraction column for the experimental conditions was calculated with the extraction rate constant $k_f = 4.26 \times 10^{-7}$ m/s, and shown as X in Fig.39 with broken lines. The observed values of X are much smaller than the calculated ones for both extractant concentrations, $C_{RH,in} = 1.78$ and 8.78 mol/m^3.

8.2.7 Extraction rate with purified extractant

When copper is extracted by LIX65N within the FISV (Takahashi and Takeuchi[57]), the extraction rates with purified extractant differs largely from those with unpurified one. And the behavior of the extraction rate with unpurified extractant within the dispersed stirred vessel coincides with that of purified extractant within the FISV. The behavior can be explained thus: the surface active impurities might affect the extraction rate and the effect might be small for the dispersed system because of the low interfacial concentration of the impurities due to the large specific interfacial area. Since the same effect of the impurities can be expected for the present extractant LIX84I, the extraction rates are measured with the purified LIX84I within the FISV. The extraction rate increases by ca. 4.5 times by the purification of extractant as shown in Fig.45, and the rate constant is given by $k_f = 1.91 \times 10^{-6}$ m/s for the purified extractant.

By using this rate constant, the outlet concentration $C_{A,out}$ from the extraction column is calculated for the experimental condition and shown in Fig.39 with solid lines. The calculated value of X agrees with the observed values. This indicates that the effect of impurities on the extraction rate might decrease with the increase in the specific interfacial area for the extractant LIX84I, too.

8.2.8 Simulation for various conditions of extraction column

The values of X calculated for various stage numbers are shown in Fig.46. The values decrease exponentially with the increase in the stage number, i.e., the counter-current multi-stage extraction is useful to remove metal ion from the dilute solution. The value of X also decreases with the increase in $C_{RH,in}$, i.e., the low copper loading ratio to extractant is effective for the copper

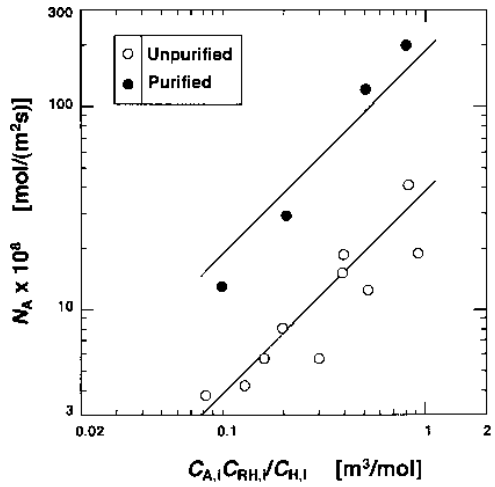

Fig.45 Comparison between extraction rates with and without purification of extractant

removal. The effects of both the continuous and the dispersed phase flow rates on X are shown in Fig.47. The calculations are carried out for a constant copper loading ratio to the extractant, $C_{A,in}Q_c/(2C_{RH,in}Q_d) = 0.15$, i.e., $C_{RH,in}$ is varied in proportion to Q_c for a given set of Q_d and $C_{A,in}$. When Q_c is small, X for small Q_d is smaller than that for large Q_d, which indicates that the increase in $C_{RH,in}$ under a given loading ratio is more effective for the copper removal than the increase in Q_d. The value of X increases with the increase in Q_c, because the extraction efficiency decreases due to the

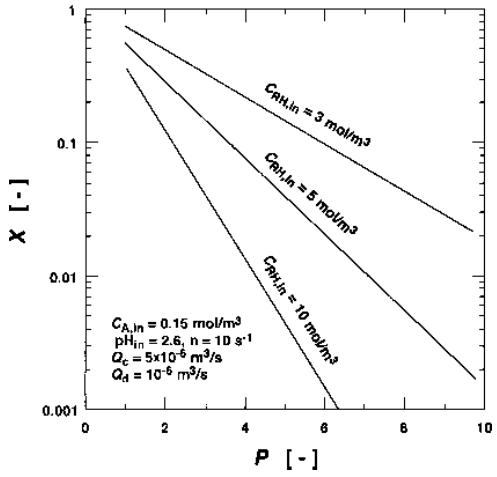

Fig.46 Calculated X for various stage number

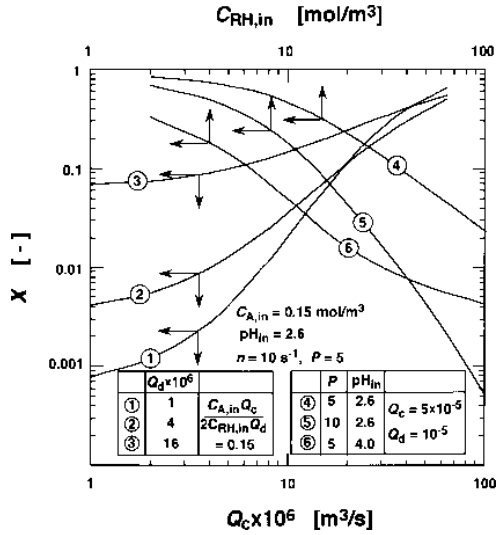

Fig.47 Effects of flow rates and extractant concentration on calculated X

decrease in the residence time with Q_c. The increase in X with Q_c is larger for smaller Q_d and the curve for $Q_d = 10^{-6}$ m^3/s went over the curves for $Q_d = 4 \times 10^{-6}$ and 1.6×10^{-5} m^3/s. This resulted from the fact that $C_{RH,in}$ increases inversely proportional to Q_d under a constant value of $C_{A,in}Q_c/(2C_{RH,in}Q_d)$, and the mass transfer resistance in the continuous phase increases with the increase in $C_{RH,in}$ as described later. In the case of the loading ratio 0.15, copper removal is small at large Q_c. Then, calculation for various $C_{RH,in}$ are carried out with relatively large Q_c ($Q_c = 5 \times 10^{-5}$ m^3/s was about half of the maximum throughput given by Nii et al.[18]) and shown in Fig.47 with lines 4, 5 and 6. The removal of copper is effective at large $C_{RH,in}$, and it is more effective with the column of large stage number ($P = 10$). When the pH of feed solution is high, $pH_{in} = 4.0$, copper is removed effectively with small $C_{RH,in}$. In addition, the decrease rate in X with $C_{RH,in}$ is small in the range of large $C_{RH,in}$, because the mass transfer resistance in the continuous phase becomes significant in this condition.

The extraction rate is expressed as follows by the use of the extraction driving force, C_A, and the total resistance, R_T, for extraction.

$$N_A = \Delta C_A / R_T = k_f C_{A.i} C_{RH.i} / C_{H.i} \tag{57}$$

When the mass transfer resistance is negligible, the extraction resistance is given by only reaction resistance, R_r, and the interfacial concentrations become equal to the bulk concentrations. Then

$$N_A = \Delta C_A / R_r = k_f C_A C_{RH} / C_H \tag{58}$$

In the same way, the following equations are obtained with the resistance $R_r + R_c$ when mass transfer resistance in the dispersed phase is negligible and $R_r + R_d$ when mass transfer resistance in the continuous phase is negligible, respectively.

$$N_A = \Delta C_A / (R_r + R_c) = k_f C_{A.i} C_{RH} / C_{H.i} \tag{59}$$

$$N_A = \Delta C_A / (R_r + R_d) = k_f C_A C_{RH.i} / C_H \tag{60}$$

Where R_c and R_d are the mass transfer resistance in the continuous phase and the dispersed phase, respectively. From Eqs.(57) - (60), the ratios of individual resistance to the total resistance are given by

$$R_c / R_T = C_{RH.i}(C_A C_{H.i} - C_{A.i} C_H) / (C_A C_{H.i} C_{RH}) \tag{61}$$

$$R_d / R_T = C_{A.i} C_H (C_{RH} - C_{RH.i}) / (C_A C_{H.i} C_{RH}) \tag{62}$$

$$R_r / R_T = C_{A,i} C_H C_{RH,i} / (C_A C_{H,i} C_{RH}) \tag{63}$$

Figure 48 shows the values of R_c/R_T and R_d/R_T within the top stage. The resistance of copper transfer within the aqueous phase increased with the increase in $C_{RH,in}$, and R_c/R_T for $pH_{in} = 4.0$ reached 0.86 at $C_{RH,in} = 100$ mol/m^3. This indicated that the mass transfer in aqueous phase was the controlling step for large $C_{RH,in}$, while the mass transfer resistance in the organic phase decreased with $C_{RH,in}$. For $pH_{in} = 2.6$, the mass transfer resistance can be considered negligible except for the aqueous resistance at large $C_{RH,in}$.

Copper is extracted by LIX84I from the dilute solution with a five-stage mixer-settler extrac-

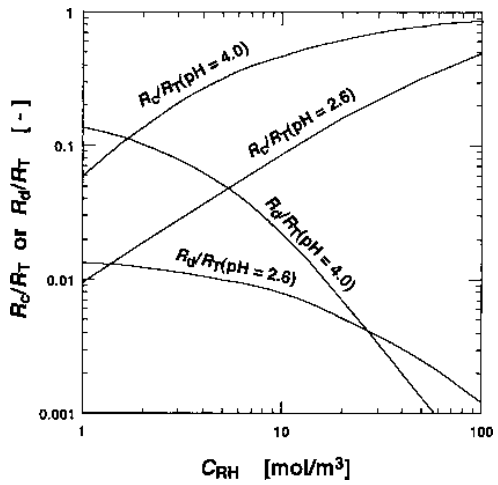

Fig.48 Ratio of mass transfer resistance to total resistance foe copper extraction

tion column. The ratio X of the outlet concentration to the inlet concentration of copper decreases largely with the agitation speed n and is 0.002 for $n = 10\ s^{-1}$ and $C_{A,in}Q_c/(2C_{RH,in}Q_d) = 0.05$. This indicates that an effective removal of copper is achieved by the extraction with multi-stage extraction column. The extraction rate of copper by LIX84I measured with a flat interface stirred vessel varies with and without the purification of extractant. The extraction rate with the purified extractant is ca. 4.5 times larger than that with the unpurified one. For the simulation of the extraction within the mixer-settler column, the calculation method taken into account the mass transfer and the extractive reaction as well as hydrodynamics is proposed. The simulated results agree well with the observed results when the extraction rate of purified extractant is used. This indicates that the effect of impurities on the extraction rate may be reduced for the dispersed system, because the interfacial concentration of surface-active impurities decreases with the increase in the specific interfacial area. The simulated results suggest that the copper removal is improved by increasing the stage number. The increase in the extractant concentration under a given copper loading ratio is more effective for copper removal than the increase in the dispersed phase flow rate, furthermore the mass transfer resistance within aqueous phase is significant only at large extractant concentrations.

References

1) Godfrey, J.C. and M.J. Slater; Liquid-Liquid Extraction Equipment, p. 227–735, John Wiley & Sons, New York (1994).
2) Sarkar, S. and C.R. Phillips; “Characterization of Hydrodynamic Parameters in Rotating Disc and Oldshue-Rushton Columns. Hydrodynamic Modeling, Drop Size, Holdup and Flooding,” *Can, J. Chem. Eng*., **63**, 701–709 (1985).
3) Kumar, A., L. Steiner and S. Hartland; “Capacity and Hydrodynamics of an Agitated Extraction Column,” *IEC Proc. Des. Dev*., **25**, 728–733 (1986).
4) Kirou, V.I., L.L. Tavlarides, J.C. Bonnet and C. Tsouris; “Flooding, Holdup, and Drop Size Measure-

ments in a Multistage Column Extractor," *AIChE J*., **34**, 283–292 (1988).
5) Komasawa, I. and J. Ingham; "Effect of System Properties on the Performance of Liquid-Liquid Extraction Column II," *Chem. Eng. Sci*., **33**, 479–485 (1978).
6) Sheibel, E.G.; "Fractional Liquid Extraction," *Chem. Eng. Progr*., **44**, 681–690 (1948).
7) Bonnet, J.C. and G.V. Jeffreys; "Hydrodynamics and Mass Transfer Characteristics of a Scheibl Extractor," *AIChE J*., **31**, 788–794 (1985) .
8) Steiner, L., E.Von Fisher and S. Hartland; "Performance of a Liquid-Liquid Extraction Column with Enhanced Coalescence Lattice," *AIChE Symp. Ser*., **80**, No.238, 130–138 (1984).
9) Gaubinger, W., G. Husung and R. Marr; "Operating Behaviour of the Self-stabilizing High Performance Extractor SHE," *Ger. Chem. Eng*., **6**, 74–79 (1983).
10) Bailes, P.J. and E.H. Stitt; *Chem. Eng. Res. Des*., **65**, 514–523 (1987).
11) Treybal, R.E.;" A Versatile, New Liquid Extractor," *Chem. Eng. Progr.*, **60**, 77–82 (1964).
12) Wirz, W.; German Patent 1918225 (1968).
13) Rincon-Rubio, L.M., A. Kumar and S. Hartland; "Characterization of Flooding in Wirz Extraction Column," *Can. J. Chem. Eng*., **71**, 844–851 (1993).
14) Horvath, M. and S. Hartland; "Mixer-Settler-Extraction Column: Mass-Transfer Efficiency and Entrainment," *IEC Proc. Des. Dev*., **24**, 1220–1225 (1985).
15) Anon: "Extractor Agitates, then Separates," *Chem. Eng*., **68**, May 1, 58–60 (1961).
16) Misek, T. and J. Marek; "Asymmetric Rotating Disc Extractor." *Brit. Chem. Eng*., **15**, 202–207 (1970).
17) Takahashi, K., H. Nakashima, S. Nii and H. Takeuchi; "Maximum Throughput in Multistage Mixer-Settler Extraction Column," *Kagakukougaku Ronbunshu*, **19**, 440–445 (1993).
18) Nii, S., J. Suzuki and K. Takahashi; "Effect of Internal Structure on Throughput of Mixer-Settler Extraction Column," *J. Chem. Eng. Japan*, **30**, 253–259 (1997).
19) Takahashi, K., S. Nii, K. Nakanishi and H. Takeuchi; "Stage Efficiency of Mixer-Settler Extraction Column," *J. Chem. Eng. Japan*, **26**, 715–719 (1993).
20) Kagakukougaku Kyoukai; Kagakukougaku Benran, 5th Ed., p. 261–264, Maruzen, Tokyo, Japan (1988).
21) Takahashi, K. and H. Takeuchi; "Interfacial Area of Liquid-Liquid Dispersion in a Mixer-Settler Extraction Column," Solvent Extraction 1990, p. 1357–1362, Elsevier, Kyoto, Japan (1992).
22) Takahashi, K. and H. Takeuchi; "Holdup of Dispersed Phase in a Mixer-SettlerExtraction Column," *Chem. Eng. Japan*, **23**, 12–17 (1990).
23) Thornton, J.D.; "Spray Liquid-Liquid Extraction Columns: Prediction of Limiting Holdup and Flooding Rates," *Chem. Eng. Sci*., **5**, 201–208 (1956).
24) Takahashi, K.; Chap.4 Drop Size and Mass Transfer in Liquid-Liquid Dispersion, Agitation and Mixing, p. 55–67, Maki Shoten, Tokyo, Japan (1990).
25) Fisher, E.A.; Dr. thesis, ETH, Zurich (1973).
26) Imai, M. and S. Furusaki; "Sauter Mean Drop Size of W/O/W Emulsions in Agitated Vessel," *Kagakukougaku Ronbunnshu*, **10**, 707–713 (1984).
27) Takahashi, K., F. Ohtsubo and H. Takeuchi; "Mean Drop Diameter of W/O and W/O/W Dispersions in an Agitation vessel," *Kagakukougaku Ronbunnshu*, **6**, 651–656 (1980).
28) Hinze, J.O.; "Fundamentals of Hydrodynamic Mechanism of Splitting in Dispersion Processes," *AIChE J*., **1**, 289–295 (1955).
29) Calderbank, P.H.; "Physical Rate Processes in Industrial Fermentation: The interfacial Area in Gas-Liquid Contacting with Mechanical Agitation," *Trans. Inst. Chem. Engrs*., **36**, 443–463 (1958).
30) Chen, H.T. and S. Middleman; "Drop Size Distribution in Agitated Liquid-Liquid Systems," *AIChE J*., **13**, 989–995 (1967).
31) Coulaloglou, C.A. and L.L. Tavlarides; "Drop Size Distributions and Coalescence Frequencies of Liquid-Liquid Dispersions in Flow Vessels," *AIChE J*., **22**, 289–297 (1976).
32) Mlynek, Y. and W. Resnick; "Drop Sizes in an Agitated Liquid-Liquid System," *AIChE J*., **18**, 122–127 (1972).
33) Vermeulen, T., G.M. Williams and G.E. Langlois; "Interfacial Area in Liquid-Liquid and Gas-Liquid Agitation," *Chem. Eng. Progr*., **51**, 85–94F (1955).
34) Konno, M. and S. Saito; "Correlation of Drop Sizes in Liquid-Liquid Agitation at Low Dispersed Phase Volume Fractions," *J. Chem. Eng. Japan*, **20**, 533–535 (1987).

34) Konno, M., M. Aoki and S. Saito; "Scale Effect on Breakup Process in Liquid-Liquid Agitated Tanks," *J. Chem. Eng. Japan*, **16**, 312–319 (1983).
35) Nnarsimhan, G., G. Nejtelt and D. Rambrishua; "Breakage Functions for Droplets in Agitated Liquid-Liquid Dispersions," *AIChE J.*, **30**, 457–467 (1984).
36) Hong, P.O. and J.M. Lee; "Changes of the Average Drop Sizes during the Initial Period of Liquid-Liquid Dispersions in Agitated Vessels," *IEC Proc. Des. Dev.*, **24**, 868–872 (1985).
37) Skelland, A.H.P. and J.M. Lee; "Drop Size and Continuous-Phase Mass Transfer in Agitated Vessels," *AIChE J.*, **27**, 99–111 (1981).
38) Bapat, P.M. and L.L. Tavlarides; "Mass Transfer in a Liquid-Liquid CFSTR," *AIChE J.*, **31**, 659–666 (1985).
39) Sada, E., K. Takahashi, K. Morikawa and S. Ito; "Drop Size Distribution for Spray by Full Cone Nozzle," *Can. J. Chem. Eng.*, **56**, 455–459(1978).
40) Tsouris, C., V.I. Kirou and L.L. Tavlarides; "Drop Size Distribution and Holdup Profiles in a Multistage Extraction Column," *AIChE J.*, **40**, 407–418 (1994).
41) Rincon-Rubio, L.M., A. Kumar and S. Hartland; "Drop-Size Distribution and Average Drop Size in a Wirz Extraction Column," *Trans. IChemE.*, **72**, 493–502 (1994).
42) Nii, S., J. Suzuki, K. Tani and K. Takahashi; "Mass Trasfer Coefficients in Mixer-Settler Extraction Column," *J. Chem. Eng. Japan*, **30**, 1083–1089 (1997).
43) Takahashi, K., M. Nakano and H. Takeuchi; "Mass Trasfer Coefficients in a Flat Type Supported Liquid Membrane," *Kagakukougaku Ronbunshu*, **13**, 256–259 (1987).
44) Kumar, A. and S. Hartland; "Mass Transfer in a Kuhni Column," *Ind. Eng. Chem. Res.*, **27**, 1198–1203 (1988).
45) Darrall, K.G. and G. Oldham; "The Diffusion Coefficients of the Tri-iodide Ion in Aqueous Solution," *J. Chem. Soc.*(A), 2584–2586 (1968).
46) Crank, J.; The Mathematics of Diffusion, p. 90–93, Oxford, UK (1975).
47) Sherwood, T.K., R.L. Pigford and C.R. Wilke; Mass Transfer, p. 25–34, McGraw-Hill, Kogakusha, Japan (1975).
48) Kagakukougaku Kyoukai; Kagakukougaku Benran, 5th Ed., p. 234–234, Maruzen, Tokyo, Japan (1988).
49) Ranz, W.E. and W.R. Marshall; "Evaporation from Drops," *Chem. Eng. Progr.*, **48**, 173–180(1952).
50) Espinola, A., L.F.M. Oliveira and F.L. Ayres; "Flow Electrolysis for Decontaminating Plate Industries Waste Water," Extr. and Proc. for Treat. and Minim. of Waste 1994, TMS, p. 369–376, San Francisco, USA (1994).
51) Tani, K., T. Ohta, S. Nii and K. Takahashi; "Copper Removal from Dilute Aqueous Solution by Extraction with Counter-Current Multi-Stage Column," *J. Chem.Eng. Japan*, **31**, 398–406 (1998).
52) Asai, S., J. Hatanaka and Y. Uekawa; "Liquid-Liquid Mass Transfer in an Agitated Vessel with a Flat Interface," *J. Chem. Eng. Japan*, **16**, 463–469 (1983).
53) Tsuboi, K., K. Takahashi and H. Takeuchi; "Simultaneous Trasfer of Two Metal Ions across Cation Exchange Membrane," *J. Chem. Eng. Japan*, **24**, 220–225 (1991).
54) Komasawa, I., T. Ohtake and T. Muraoka; "Extraction Kinetics of Copper withHydroxyoxime Extractant," *J. Chem. Eng. Japan*, **13**, 204–208 (1980).
55) Takahashi, K. and H. Takeuchi; "Stripping Rates of Copper for LIX65N-Copper System," *Kagakukougaku Ronbunshu*, **10**, 543–544 (1984).
56) Davies, G.A.; Science andPractice of Liquid-Liquid Extraction, J.D. Thornton(ed.), p. 247–252, Oxford, UK (1992).
57) Takahashi, K. and H. Takeuchi; "Rates of Copper Extraction by LIX65N," *Kagakukougaku Ronbunshu*, **10**, 409–414 (1984).